Noman Nisar

Structural Optimization and Thermal Modeling of Flux Switching Machine

School of Electrical Engineering

Master's Thesis submitted in partial fulfillment of the requirement for the degree of Master of Science in Technology.
Espoo

Thesis supervisor:

Prof. Antero Arkkio

Thesis instructor:

D.Sc. (Tech.) Vicente Climente-Alarcon

M.Sc. (Tech.) Sahas Bikram Shah

Aalto University
School of Electrical
Engineering

Aalto University School of Electrical Engineering Master's Programme in Electrical Engineering	ABSTRACT OF THE MASTER'S THESIS

Author: Noman Nisar		
Title: Structural Optimization and Thermal Modeling of Flux Switching Machine		
Number of pages: 9+64	Date: 2-12-2014	Language: English
Professorship: Electromechanics		Code: S-17
Supervisor: Prof. Antero Arkkio		
Instructors: D.Sc. (Tech.) Vicente Climente-Alarcon M.Sc. (Tech.) Sahas Bikram Shah		

The point of this study was to model a lumped parameter thermal network for flux switching machine. The model could be utilized to outline new cooling systems and as a developer for this sort of machines. The model developed is a thermal framework having segments essentially focused around existing literature. The losses in various machine sections were thought to have already found from the electromagnetic model. The elemental model can then be utilized to carry out simulations regarding cyclic loading as well as transient activities. The thermal model examined here is partitioned into different sectors, thereby empowering analysis of this machine.

The model under investigation has been acknowledged by utilizing a COMSOL Multi-physics simulator and Matlab ® programming software. The heat exchange coefficients are characterized from information gathered from the comparative kind of machines. The developed framework also considers sensitivity analysis in terms of parametric effects on the behavior of the machine thermally. The developed model needs no substantial computing and can simply be run on a personal computer. The model can later be modified and connected to diverse machine developments.

Structural topology optimization approach is adopted to find the optimal geometry. As a basic study, two optimization techniques i.e., genetic and simulated annealing algorithms have been adopted with the former based on the process of natural selection and the latter on the process of annealing (heating and cooling of metals). The design goal is to minimize the total dissipated losses to improve the overall efficiency and hence to achieve optimal design results.

Keywords: flux switching machine, FEM, optimization, thermal resistance network, thermal modeling

Preface

This master thesis was carried out in Electromechanics research group at School of Electrical Engineering, Aalto University. This research work is the part of the research project *Empathy* and I would like to thank the representatives for their financial support.

First and foremost, I would like to express my deep gratitude to my supervisor **Prof. Antero Arkkio** and my instructors **Vicente Climente-Alarcon** and **Sahas Bikram Shah** for their patient guidance, enthusiastic encouragement and useful discussions. I would also like to appreciate the encouragement of Prof. Anouar Belahcen during my research work.

Besides, I would like to thank Mr. Ari Haavisto for his technical assistance. I am also thankful to all my colleagues in Electromechanics research group for creating pleasant working environment. I am especially thankful to Bishal Silwal for helping me in proof reading of my thesis.

Last but not least, I would like to express my heartfelt thanks to my parents for their ceaseless blessings, love and support. I would also like to thank all my friends and relatives for always being there for me.

Otaniemi, 2.12.2014

Noman Nisar

Contents

Symbols and Abbreviations

Roman Letters

A	Surface Area
c	Specific heat capacity
C	Capacitance
d	Characteristic dimension of the system
E	Electric field
f	Objective /fitness Function
g	Acceleration due to gravity
G	Conductance
$\boldsymbol{G}$	Conductance matrix
h	Heat transfer coefficient
$\bar{h}$	Average heat transfer
h_{V}	Vertical heat transfer coefficient
h_{H}	Horizontal heat transfer coefficient
I	Current intensity
J	Current density
k	Thermal conductivity
K_{c}	Empirical constant
l	Length or distance
L	Characteristics length (Distance between the faces)
m	Mass
$\boldsymbol{n}$	Unit vector normal to the surface
P	Power loss, heat flow
$\boldsymbol{P}$	Power loss vector
$\boldsymbol{P}_{\mathrm{u}}$	Loss vector containing injections at node points
p	Pressure
q	Heat flux
q_G^*	Rate of heat generation per unit volume
Q	Heat
Q_{rod}	Empirical constant which depends on the geometry of coil and core
r	Radius

R	Resistance
S	Area of transversal section
T	Temperature of fluid, T_∞; temperature of region far from the surface; T_{fl}, temperature of bulk of fluid; T_{s}, surface temperature
u	Velocity field
V	Potential
V	Volume
v	Velocity of medium
x	Design variable
y	State variable

Greek Letters

α	Thermal diffusivity $= k/\rho c$
β	Coefficient of thermal expansion
δ	Skin depth
ε	Emissivity
η	Dynamic viscosity
θ	Temperature rise
$\boldsymbol{\theta}$	Temperature rise vector
λ	Thermal conductivity
μ	Magnetic permeability
ν	Kinematic viscosity
ρ	Mass density
ρ_{r}	Resistivity
σ	Conductivity
φ	Angle of a segment
ω	Angular frequency

Dimensionless Numbers

Gr	Grashof number
Nu	Nusselt number

Pr	Prandtl number
$R_{e\delta}$	Reynolds's number
T_a	Taylor number

Subscripts and Abbreviations

2-D	Two dimensional
3-D	Three dimensional
av	Average
CFD	Computational Fluid Dynamics
D	Conduction
el	Electrical
FEM	Finite Element Method
FSPM	Flux Switching Permanent Magnet
ga	Genetic Algorithm
MHu	Horizontal upper section of Magnetic Holder
MH	Magnetic holder
ODE	Ordinary Differential Equation
PDE	Partial Differential Equation
PM	Permanent Magnet
R	Rotor
RS	Rotor-Stator
SO	Structural optimization
th	Thermal
TEC	Thermal Equivalent Circuit
V	Convection
W	Windings

Page left intentionally

1. Introduction

The use of hybrid vehicle frameworks has experienced a rapid growth in popularity in a short span of time and it seems to have a promising future. One range where exertions are, no doubt guided at specialized changes is the region of interest between the thermal and electrical parts of motors. There are of course advantages associated to know more about the conduct and the impacts of the heat created in the machine while it is in running condition. It is therefore of extraordinary importance to verify that the temperature does not reach its thermal limits, particularly for delicate and sensitive parts. For machines utilized within situations where cooling is extremely difficult, particularly for hybrid machines, this comprehension is maybe even more important.

1.1 Problem Statement

The thermal limit imposes restrictions on the machine. Go past them and they will decrease the life expectancy of the motor and ultimately a large portion of the capability of the machine will be wasted. If such restrictions can be considered as soon as possible in the optimization methodology, it is conceivable to accomplish a more homogeneous temperature variation and we can then avoid problem areas that might occur inside the machine. The obtained information could be helpful for enhancing the general requirements regarding effectiveness, torque/power density, optimization and necessities on the cooling [1]. Having good information about the thermal limits of the machine implies; having the capacity to plan the design in a cost effective way without considering the available gap thermally before the upper limits could be reached.

Various existing publications describe distinctive parts of the thermal modeling of electric motors. On flux switching machines with PM's however, little information is available. By considering the detailed model, there can be a lot of questions that needs to be addressed. A closer examination of modeling the flux switching machine is specifically interesting, as it is the kind of electrical machine employed as a part of the new emerging technologies.

The model ought to be parametric in terms of thermal resistances and the parameters should be swept within reasonable interval gap depending upon the accuracy of the variable selected. From this information, the most important and relevant variables can be distinguished and therefore the criteria for outlining the thermal parts of an electric machine can be specified.

Since the thermal model of the machine under consideration is parameterized, it is general enough to apply the same for researching different motor designs.

1.2 Literature Review

There are various types of thermal model networks and researchers have done a lot of research and have published articles on the concerned topic of thermal modeling. The basic principles are the same in every type of machine, except different type of structures and topologies. I have studied the articles written by Kaltenbacher & Saari [19], T. Jokinen [11] and Kylander [1] which describes the thermal modeling of electrical machines in great depth. Especially in high-speed machine product development, thermal models have been an important tool till 1995, as the power densities and losses were significant at that time. Air flow cooling effects have been studied a lot by A. Bousbaine and M. McCornick [14], Gazley, C. [16] and Luke, G.F. [26]. [9], [12], [13] have discussed the thermal behavior of axial flux machines and have also presented simplified thermal resistance

networks for an axial-flux PM machine. Flux switching machine development is so new that the established analytical models do not just exist.

1.3 Purpose and Work Scope

The motivation behind this study is to create a thermal resistance framework for flux switching machines. The machine considered here has low number of tooth pairs in the stator and has permanent magnets. In that respect it varies from the motors displayed in the dominant part of published articles nowadays, which may imply that conventional systems may not generally be the ideal. Since the effect of heat flowing in the axial direction is by and large viewed as negligible, the system is restricted to consider only circumferential and radial heat flows. For verification, a finite element based model is created using software tools to compare the results of FEM with the developed analytical model.

The framework developed should explain the questions about the behavior of electrical machines thermally. Research should also be made on how the temperatures in diverse parts of the machine are linked with some geometrical properties. A few conclusions can be drawn from this analysis regarding which variables in the design process are vital for the temperature distribution and at what part of the machine consideration should to be taken because of the parametric variations. The motive of this research project was to develop a thermal network incorporating thermal modeling of distinctive parts of the specific machine and the calculations involved in assessing the heat transfer coefficients in various parts of the machine.

The idea of modeling and thermal simulation of electrical machines demands such complicated questions that cannot all be answered adequately considering the time span of thesis concerned. Losses in the motor and electromagnetic characteristics of the machine are two such assumptions that need to be considered thoroughly. The scope of this thesis does not deal with these areas in depth.

1.4 Methodology

The framework has been produced iteratively, beginning with less complex model and considering just the fundamental parts. Correctness and points of interest were included as the information of the other key elements and difficulties expanded. Already built techniques are generally analyzed at the start and can sometimes be reproduced directly using the already build methodologies. Alternatively some innovative thoughts can be tried with the plan of enhancing correctness or essentially adjusting the parameters, which describe the concerned motor more effectively.

To check the credibility of the thermal model developed, the same analysis is performed by finite element method in addition to the thermal resistance network. The obtained results from either method should be predictable and the similarity between the two techniques should also give a sign to the accuracy of the results.

Despite the fact that the FEM result has the capability of being extremely detailed and precise, it can't be more accurate than the input data information itself. If suppositions about the properties for example, interface gaps, materials, properties of air etc. have some discrepancies, these blunders will be reflected in the output simulation. Besides, the software used is constrained in considering all liquids as solids, implying that the same technique for modeling air gap convective coefficients will be deployed in the software as in case of solids. In other words, the finite element

method cannot be considered as to give completely reliable results, but just to provide us with information that can be validated by experimental results.

1.4.1 Configuration of Program and Simulation Concerned

It is critical to verify that both methods of modeling reliably investigate the same operating conditions of the motor. For this reason high accuracy is required to verify that all the arrangements are effectively available and to as substantial degree as could also reasonably assembled at one place. This influences convenience, however more importantly it brings down the danger of contrasting results from the two diverse models when different settings are compared.

The modeling of thermal framework is coded in Matlab ®. The generalized program shows that different input parameters can be executed and can be called in other sub routines. Setting of the parameters and the layout of the program, for example, input data of the machine including important variables and temperature distribution by iteration are carried out in the main file. The output gives the resulting temperatures of various parts of the machines.

The FEM-simulations have been carried out in COMSOL Multiphysics software suite "heat transfer in solids (ht)" and "heat transfer in fluids". The (ht) module has nodes for "thermal insulation", "electric current (ec)" and "initial values" in which heat flux and heat source terms have been defined. The heat transfer in solids (ht) and electric current (ec) nodes have settings for heat conduction and current conduction respectively.

- Under electric current node, current conservation represents the conservation of electric current at domain level.

- Electric Insulation node contains the boundary conditions for electric currents.

- Under heat transfer in solids (ht) node, the domain level node represents the conservation of heat and the thermal insulation node defines the boundary conditions for heat transfer (without taking into account the weak expressions).

Thermal insulation actually is a depletion of heat exchange (the energy exchange in the form of heat between the objects of contrasting temperatures) between objects which have thermal links with each other or in the scope of radiative impact. It gives a section of insulation where thermal conduction is decreased or radiation is ignored as opposed to absorbed by low temperature body. The capability of insulating material is judged with thermal conductivity k, lower value of which is proportional to high level of insulation. In electrical engineering, other characteristics of insulating materials that are considered important apart from thermal conductivity are density ρ and specific heat capacity c.

2 Background of Thermal Modeling

Thermal modeling is about describing the thermal conduct of a system by utilizing the scientific and methodological means. It allows one to answer inquiries about how high the temperature will be dispersed and will respond to the changes considering the properties of the material and geometry of the machine.

Thermal networks are comparable with electrical circuits [2]. This implies that the comparisons and constraints on the boundary describing a particular system could be utilized to portray the other system by just replacing the variable symbol, and then all fundamental electrical circuit laws can be applied satisfactory for thermal systems as well. The relationships between few quantities of electrical and their analogy with thermal quantities are shown in Table 1.

As in the scope of this thesis we will often use thermal terminologies, the subscript "th" will not be used later on, for the sake of convenience.

Table 1: Relationship between some Electric and Thermal Quantities

Electrical quantities			*Thermal quantities*		
Potential	V	[V]	Temperature	θ	[°K]
Current	I	[A]	Heat	Q	[W]
Current density	J	[A/m^2]	Heat Flux	q	[W/m^2]
Conductance	G_{el}	[S]	Thermal conductance	G_{th}	[W/K]
Conductivity	σ_{el}	[S/m]	Thermal conductivity	$k \sim \lambda$	[W/mK]
Resistance	R_{el}	[Ω]	Absolute thermal resistance	R_{th}	[K/W]
Resistivity	ρ_{r}	[Ω/m]	Absolute thermal resistivity	$\rho_{\mathrm{r,th}}$	[mK/W]
Capacitance	C	[F]	Thermal capacitance	C_{th}	[J/°K]

2.1 Mechanisms of Heat Exchange

The second law of thermodynamics states that there is constant net entropy expands in real methodologies and processes. Entropy is frequently explained in literatures as chaos or disorder in a framework, which can likewise be utilized to portray the measure of the system energy, with low level points in the direction of high disorder. In this manner, the same law could additionally be clarified by explaining that an isolated framework dependably looks for thermal balance. Or even simply, heat will flow from a place high in temperature to a cool place [3].

Heat exchange can take place through three mechanisms. These are heat conduction, convection and radiation [3]. Few equations have been designed to model these heat exchange mechanisms [2], [3], [4]. By the help of these formulas and the similarity between electrical and thermal networks, a thermal model for a particular machine type can be designed [19].

Conduction is referred to as propagation of energy among particles in a channel. Besides being the only method for the exchange of heat in solids, it is not entirely linked to it, but happens in fluids as well. The conduction equation is specified by Fourier's Law.

For 1-D problems, Fourier's law is given as

$$q''_{\mathrm{x}} = -k\frac{dT}{dx} \qquad (1)$$

q'' in the above expression is the heat flux per unit area with subscript "x" indicates the direction of interest. k is the constant of proportionality referred to as thermal conductivity and $\frac{dT}{dx}$ is the temperature gradient at a particular location. The negative sign indicates that heat flows to a point where there is a net decrease in temperature gradient.

In fluids and gases, we can also find the phenomena of convection. As the particles in the channel are allowed to move freely, the heat exchange capability of the channel is enhanced by the movement of the particles themselves, intermixing particles of distinctive levels of energies and expanding the rate of collision with others. Similar to conduction, the equation for convection is represented by Newton's Law as

$$q'' = h(T - T_{\infty}) \qquad (2)$$

Where h is the heat exchange coefficient, T is the temperature of the solid surface and T_{∞} is the temperature of the cooling medium away from the surface. The relation mentioned above is a numerical expression of the heat power i.e., heat flux per unit area and the temperature gradient across the solid surface and cooling fluid medium. Experimental data are required for validating the values of heat exchange coefficients.

The last and the final mechanism is that of radiation which explains the phenomena of a body releasing energy particles called photons. The quantity a body releases radiation is linked to the emissivity of the body, the cross sectional area of the surface and most importantly on the temperature [4]. The equation below describes the total exchange of energy in the form of heat as

$$q'' = \varepsilon\sigma\left(T_{\mathrm{i}}^4 - T_{\mathrm{j}}^4\right) \qquad (3)$$

Where ε is the emissivity of the system, σ is a constant of Stephan-Boltzmann 5.67 x 10^{-8} $(\frac{\mathrm{W}}{\mathrm{m^2K^4}})$ and $(T_{\mathrm{i}}^4 - T_{\mathrm{j}}^4)$ is the difference of temperature between two systems to the fourth or higher power.

In electrical machines, mechanisms like radiation and convection are linked to the air gap heat transfer and the ambient thermal effects. The radiation effect is usually small for electrical machines [5] and will therefore not be considered in this thesis.

Furthermore, the methodology of predicting the movement of fluids can be exceptionally complex and time intensive. About modeling of air, this thesis will not point out detailed investigation on this, rather will use already established methods in previous publications. In this way the difficulty to the problem can be lowered while considering mainly the geometrical sections.

2.2 The Heat Transfer Theory

The heat generated in electrical machines is actually an after-effect of the transformation of electrical and mechanical losses (hysteresis, eddy current, ohmic and friction losses) to heat. In general, there exists a heat flow from the inner to the outer parts of the electrical machine [19]. The heat is transferred usually from upper potential to lower potential as an electric current. It may be

transmitted via conduction, radiation or convection. Thermal network is comprised of familiar circuit segments as has already been defined in the Table 1, followed by the theory which is mainly based on sources referred by [2], [3] and [20].

2.2.1 Conduction

Conduction through solids is a mechanism of heat exchange. The basic idea was given by French scientist J. Fourier in 1822, especially known throughout the world as Fourier's Law [28]. For a 1-D geometrical figure, this is given as in (1) and has been reproduced here as

$$q_{\mathrm{k}} = -kA\frac{dT}{dx} \qquad (4)$$

Where q_{k} is the conduction heat transfer rate (i.e., heat flux) passing the surface area A as shown in Figure 1, $dT = t_1 - t_2$ is the temperature difference, dx is plate wall distance and k is the proportionality constant known as the thermal conductivity of the plate material in $\frac{\mathrm{W}}{\mathrm{mK}}$. The value of k varies for different materials and one being typical value for conductivity of air is $0.026\ \frac{\mathrm{W}}{\mathrm{mK}}$ [27].

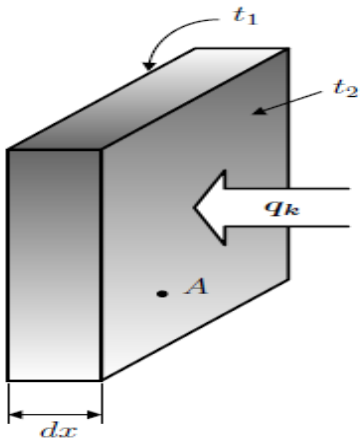

Figure 1: Conduction phenomena by Fourier's law implemented to the 1-D plane geometry [3]

The minus sign in (4) is inserted so as to satisfy thermodynamics' second law i.e., heat flux must decrease on the temperature scale in the heat flow direction [22] [27]. In other words, the rate of heat exchange is taken to be positive in the direction of decreasing temperature as indicated in the coordinate system of Figure 2.

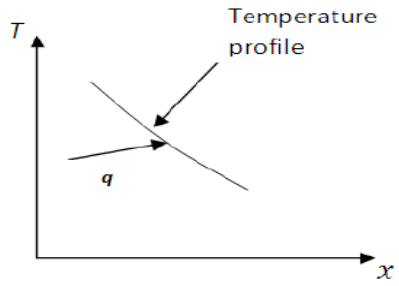

Figure 2: Direction of heat flow [3] [28]

However (4) does not consider all energy but just the energy infused into a plate. To get a differential conduction mathematical statement, energy conservation principle ought to be implemented. The equation for 1-D heat exchange by the phenomena of conduction, derived from various articles is simply given here as

$$k\frac{\partial^2 T}{\partial x^2} + q_{\mathrm{G}}^{*} = \rho c\frac{\partial T}{\partial t} \tag{5}$$

ρ in this expression is the density of the material and c is the material's specific heat or thermal capacity.

The first term on the left side gives the volumetric heat flow rate. The second term is internally produced per unit volume of energy and the right side describes the volumetric internal energy change. The expression in (5) assumes heat conductivity to be constant i.e., it is not a function of spatial coordinates or temperature.

The derivation of (5) is based on the supposition that the temperature distribution is 1-D. If this condition is removed, temperature depends on all three dimensions as well as on time i.e. $T = T(x, y, z, t)$. The conduction equation for a three-dimensional control volume given in Figure 3 is expressed as

$$\frac{\partial^2 T}{\partial x^2} + \frac{\partial^2 T}{\partial y^2} + \frac{\partial^2 T}{\partial z^2} + \frac{q_{\mathrm{G}}^{*}}{k} = \frac{1}{\alpha}\frac{\partial T}{\partial t} \tag{6}$$

Where α is the thermal diffusivity defined as

$$\alpha = \frac{k}{\rho c} \tag{7}$$

For a stationary problem, the temperature of the material is not time dependent, i.e. $T = T(x, y, z)$ and the right term of (6) can therefore be ignored. The steady-state form of the three-dimensional heat conduction equation is

$$\frac{\partial^2 T}{\partial x^2} + \frac{\partial^2 T}{\partial y^2} + \frac{\partial^2 T}{\partial z^2} + \frac{q_{\mathrm{G}}^{*}}{k} = 0 \tag{8}$$

If no heat is generated internally, the conduction equation has a form of

$$\frac{\partial^2 T}{\partial x^2} + \frac{\partial^2 T}{\partial y^2} + \frac{\partial^2 T}{\partial z^2} = 0 \tag{9}$$

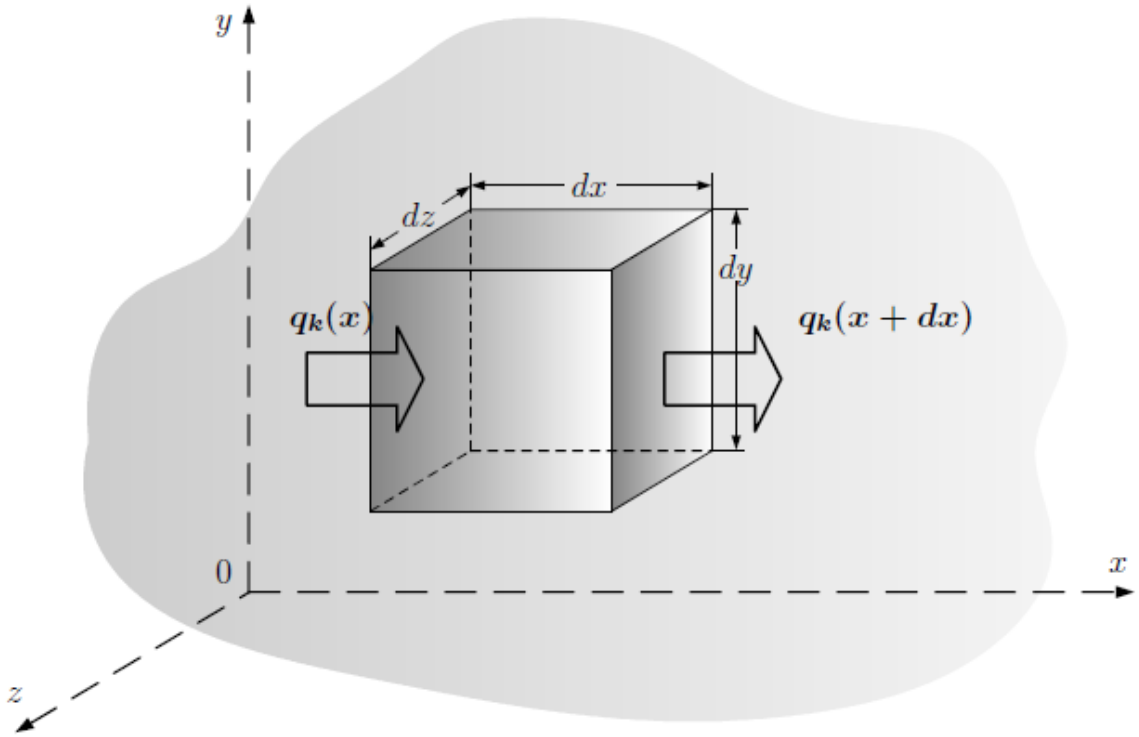

Figure 3: Control volume for three dimensional conduction [27]

2.2.2 Convection

In convection mode, heat is exchanged with varying temperature that exists between the surface of a body and the surrounding medium. The heat exchange mechanism in convection comprises of two components working at the same time: heat conduction and cooling media transport. The cooling medium movement is a consequence of force exerted by some external means, especially in the case of forced cooling machines. Depending on the nature of external medium which exerts the force, convection might be named as either forced, created by a fan or a pump, or natural because of the varying density of the medium.

The rate of heat transfer by convection between corresponding surface and fluid is determined by Newton's Law of Cooling [27] as has already been defined in (2)

$$q = \overline{h_{\text{conv}}}\, A\, \Delta T \qquad (10)$$

ΔT is the difference between the surface temperatures and ambient temperature, $\overline{h_{\text{conv}}}$ is the average heat transfer coefficient over surface area A (subscript "conv" in $\overline{h_{\text{conv}}}$ refers to convection). The value of $\overline{h_{\text{conv}}}$ varies from 6 $\frac{\text{W}}{\text{m}^2\text{K}}$ for natural air convection to 120000 $\frac{\text{W}}{\text{m}^2\text{K}}$ [27].

A quantitative assessment of convection heat transfer coefficient is a complex issue as $\overline{h_{\text{conv}}}$ depends on many variables like geometry of the surface, flow characteristics, flow velocity, physical properties of a fluid and temperature difference ΔT. The estimation of heat exchange coefficients

can likewise differ along the cooling or heating surface [27]. However, for most engineering applications, the average value of h_{conv} is often used instead.

2.2.3 Laminar Flow Energy Conservation Equation

The principle of conservation of energy is applied to obtain the heat equation that matches the velocity field u and the temperature T. This can be used as a boundary condition to the problem concerned. The energy conservation equation in vector notation is given by [28] as

$$\rho c_p \frac{\partial T}{\partial t} + \nabla.\left(-k\Delta T + \rho c_p T u\right) = q \qquad (11)$$

Where ρ in this expression is the density, c_p is the thermal capacity of the cooling medium at constant pressure. The expression within the brackets is the heat flux vector and q on the right side represents the heat flux i.e., the heat source term.

2.2.4 Evaluation of Convective Heat Transfer Coefficients

As indicated in [28], broadly five general routines can be described for the assessment of convective heat exchange coefficients:

1. *Dimensional analysis with investigations* is numerically basic system which is generally utilized for assessment of high heat exchange coefficients. However, the results from these are rather ambiguous and cannot be used without having comparison with some sort of experimental results.

2. *An accurate scientific result of the boundary layer equations* is numerically unpredictable and mathematically complex system, which requires the simultaneous solution of the equations describing the motion of cooling fluid and transfer of heat due to this moving fluid.

3. *Approximate analysis of the boundary-layer equations by integral method* is moderately a straightforward method, which stays away from the definite scientific description of the cooling medium. The mathematical equation of motion and the energy equation is coupled together simultaneously to evaluate the heat exchange coefficients.

4. *Relationship between heat and momentum* $(energy)$ *exchange* is a method used to analyze the turbulent flow of the cooling fluid.

5. *Numerical analysis* is a technique used to solve the exact equations of motion. An important advantage of this method is that once the solution to a particular problem has been outlined, an approximate analysis of boundary layer equations can easily be evaluated.

The thermal resistance unit in general sense is,

$$[R] = \frac{[l]}{[\lambda][A]} = \frac{\mathrm{m}}{\left(\frac{\mathrm{W}}{\mathrm{mK}}\right)\mathrm{m}^2} = \frac{\mathrm{K}}{\mathrm{W}} \qquad (12)$$

Power is supplied to the resistor by means of ohms law. Similarly, the power flow through the resistor R having a point temperature θ is given as

$$P = \lambda \frac{A}{l} \theta = \frac{\theta}{R} \tag{13}$$

In other words, the point obtained by the temperature θ of the power loss P caused by the heat flow and the thermal resistance R is written as of (13)

$$\theta = RP \tag{14}$$

In this case, θ describes the thermal environmental temperature in relation to a point where they are imported, P is the power loss and the ambient temperature level of resistance is R.

Q_{th} corresponds to the electronic model of the capacitor charge Q_{s}. The relationship is expressed as

$$Q_{\text{th}} = mc_p\theta \tag{15}$$

Where m is the mass, c_p is the specific heat capacity at constant pressure and θ is the point temperature.

The heat capacitance is defined as

$$C = V\rho c_p \tag{16}$$

2.2.5 Thermal Resistance of Solids

Not like the properties of mass or conductivity, thermal resistance of an item is computed keeping in view the direction of heat stream [1].

The thermal conductance can be calculated by (13)

$$G = \frac{1}{R} = \lambda \frac{A}{l} \tag{17}$$

λ is the thermal conductivity, A is the cross sectional area and l is the distance between the nodes.

Accordingly, the thermal resistance is

$$R = \frac{1}{G} = \frac{l}{\lambda A} \tag{18}$$

If the area of a conductor is to vary over length l, then the resulting integral is expressed as

$$R = \int_o^l \frac{dl_{\text{p}}}{\lambda A(l_{\text{p}})} \tag{19}$$

Where p in the subscript of l_{p} denotes the path length. This is the basic expression from which most resistances for the use in thermal network modeling can be deduced.

2.2.6 Thermal Resistance of Gases and Fluids

At far as the point of representation of air in thermal network is concerned, convection is a heat exchange process that needs to be considered. The modeling of air is a complex task since fluid movement depends on variety of variables for example, rotational speeds, surface structure, geometrical dimensions, heat flows and so on. The thermal resistance between solid and ambient is written as

$$R = \frac{1}{hA} \tag{20}$$

Where A is the cross sectional surface area subjected to convection and h is the heat exchange coefficient. The SI unit of heat transfer coefficient is watts per squared meter kelvin $\left[\frac{\mathrm{W}}{\mathrm{m^2K}}\right]$.

Finding the values of convective heat transfer coefficient h is somewhat challenging as it requires extensive information about the machine concerned. Having some good estimated values also requires detailed knowledge on subjects like Computational Fluid Dynamics (CFD), a FEM based method, which demand lot of skills and efforts. Such itemized learning is however not generally a prerequisite [5] rather, it is frequently computed by utilizing equations focused around empirical studies. The behavior of the air movement can be described by few dimensionless numbers described in section 2.3.

2.3 Dimensional Analysis

Dimensional investigation involves few variables to form various dimensionless numbers. The primary disadvantage of this technique is that the results acquired from the calculations are either ambiguous or truly pointless unless verified by some sort of experimental results. In addition, the quantity of variables affecting the physical methodology of heat exchange ought to be chosen beforehand. Nevertheless, once the important variables are known, dimensional analysis can then be applied to general issues.

2.3.1 Nusselt Number

The Nusselt number (Nu), "ratio of convective to conductive heat transfer normal to the boundary", is perhaps the one most closely related to the heat transfer coefficient [32].

The relationship between the heat transfer coefficient and the Nusselt number is expressed as

$$h = \frac{\lambda_{\mathrm{air}} Nu}{2l} \tag{21}$$

The Nusselt number in general can be written as in [19]

$$Nu = \frac{h_{\mathrm{c}} d}{\lambda} \tag{22}$$

Where h_{c} $[\mathrm{Wm^{-2}K^{-1}}]$ is the heat transfer coefficient of convection. d [m] is the characteristic dimension of the system and λ $[\mathrm{Wm^{-1}K^{-1}}]$ is the thermal conductivity.

A Nusselt number (Nu) of value "2" corresponds to a laminar flow [2]. "The convection and conduction heat flows are parallel to each other and to the surface normal of the boundary surface,

and are all perpendicular to the mean fluid flow" [32]. When that is the case, (20) becomes the same as for any solid, which is seen if inserting (21) in (20). Nusselt number tends to be higher for high rotor speeds and uneven surfaces, since because of these effects the turbulence increases.

2.3.2 Reynolds Number

It is defined as a "ratio of inertial to viscous force" [32]. The Reynolds number is expressed as

$$R_{e\delta} = \frac{\rho v^2}{\eta \frac{v}{d}} = \frac{vd}{\nu} \tag{23}$$

Where ρ [kgm^{-3}] is the mass density, η [kgm^{-1}s^{-1}] is the dynamic viscosity, ν (Ny) [m^{2}s^{-1}] is the Greek symbol of kinematic viscosity, d [m] is the characteristic dimension of the system and v [ms^{-1}] is the velocity of the cooling medium.

2.3.3 Prandtl Number

It is a "dimensionless ratio of the viscous boundary layer thickness to the thermal boundary layer thickness". The Prandtl number [32] is defined as

$$Pr = \frac{\nu}{\alpha} \tag{24}$$

Where ν (Ny) is the kinematic viscosity and α is the thermal diffusivity for transport of thermal energy due to friction [19].

2.3.4 Grashof Number

It is defined as a "ratio of hydrostatic and viscous force" [32] given as

$$Gr = \frac{\beta g \Delta T d^3 \rho}{\nu^2} \tag{25}$$

β [K^{-1}] in this expression is the coefficient of thermal expansion, g [ms^{-2}] is the gravitational constant, ΔT is the temperature difference between surface and cooling medium, d [m] is the characteristic dimension of the system, ρ [kgm^{-3}] is the mass density and ν (Ny) [m^{2}s^{-1}] is the kinematic viscosity.

Formulas of heat transfer caused by free convection are set up as a function of Grashof and Prandtl number and in case of forced convection by Prandtl and Reynolds number.

2.4 Strategic Heat Transfer Problems

Two methods for taking care of heat exchange issues have been described in the scope of this thesis. First is the Thermal Resistance Network Modeling which is a strategy mainly focused around the basic heat exchange for simple machines and second is more computational Finite Element Method, which is close to exact, provided good input data.

2.4.1 Network Solution

As mentioned earlier, the thermal network is like an electronic circuit which can be seen by considering the thermal network example of Figure 4.

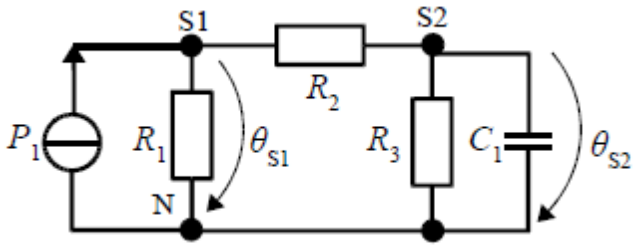

Figure 4: Thermal network example [20]

Of the various possible solution methods, the node method which is based on thermal resistance network modeling is the most convenient way when using a computer to solve. The zero level will be selected usually for the ambient temperature, whereas the potentials of the nodes corresponding to warming up their relation to the environment are represented by conductance's i.e. the inverse of the resistances.

2.4.2 Modeling of Thermal Resistance Framework

To discover the steady state conduct of a thermal framework, it may be identified by a network containing thermal resistances, heat flows and temperature sources (Figure 4). The conductance matrix of a whole system involving n + 1 node points can be written in mathematical form as

$$\boldsymbol{G} = \begin{bmatrix} \sum_{i=1}^{n} \frac{1}{R_{1,\mathrm{i}}} & -\frac{1}{R_{1,2}} & \cdots & -\frac{1}{R_{1,\mathrm{n}}} \\ -\frac{1}{R_{2,1}} & \sum_{i=1}^{n} \frac{1}{R_{2,\mathrm{i}}} & \cdots & -\frac{1}{R_{2,\mathrm{n}}} \\ \vdots & \vdots & \ddots & \vdots \\ -\frac{1}{R_{\mathrm{n},1}} & -\frac{1}{R_{\mathrm{n},2}} & \cdots & \sum_{i=1}^{n} \frac{1}{R_{\mathrm{n},\mathrm{i}}} \end{bmatrix} \tag{26}$$

Let $\boldsymbol{P}$ be the power loss vector which represents the losses inserted in various node points as

$$\boldsymbol{P} = \begin{bmatrix} P_1 \\ P_2 \\ \vdots \\ P_n \end{bmatrix} \tag{27}$$

And temperature vector is

$$\boldsymbol{\theta} = \begin{bmatrix} \theta_1 \\ \theta_2 \\ \vdots \\ \theta_n \end{bmatrix} \tag{28}$$

These matrices can be written as

$$\boldsymbol{G}\,\boldsymbol{\theta} = \boldsymbol{P} \tag{29}$$

So, θ can be calculated by the inverse of conductance matrix and simply multiplying it with the power loss vector which results in

$$\boldsymbol{\theta} = \boldsymbol{G^{-1}P} \tag{30}$$

As we know setting up an exact thermal model requires some complex working but the model developed in this way gives a method for getting quick answers for variations in input parameters, since by this way the numerical complexity and number of fundamental proceedings can be kept low. The time taken to set up the model relies upon the level of points of interest i.e., on the nodes and also on the accuracy required for designing a reliable model [2]. The methodology for finding out thermal resistances for some general geometrical shapes is depicted in later sections.

2.4.3 Finite Element Analysis

FEM is an extremely important and intensive tool in elementary frameworks, for example, structural mechanics and thermodynamics [6]. Scientifically, such a framework can also be described by differential equations, which at times becomes difficult to solve and explain. It is therefore required to have a technique for making the issues less complicated while also having the capacity to withstand the neighborhood impacts.

The fundamental guideline is that such a framework is partitioned into various manageable and generally characterized components. If such small various elements are allowed to grow and approach infinity, then this would correspond to such a continuous network that would no doubt be very reliable but practically also very difficult to solve. A numerical result can then be gained when these individual component equations have been gathered into a single framework and solved simultaneously in TEC.

In the case of FEM simulations in this thesis, we will essentially solve the equation of conduction presented in 2.2.1.

2.5 Methods of Modeling Thermal Network

At the point when a thermal resistance network has been built up, there are numerous inquiries for example, how to simplify the item being referred to, where to place the nodes and how comparable thermal resistances could be, while solving for distinctive shapes. This section presents principles and equations for developing a thermal network. Important parts of the machine to be considered in the heat transfer i.e., in the thermal modeling of the machine are

- Rotor iron
- Permanent magnets

- Stator bars
- Stator winding
- Air gap
- Magnetic holder

The thermal framework in a steady state comprises of thermal resistances and sources which represent heat associated between various motor segment hubs (nodes). As for transient case examination, thermal capacitances are also utilized to consider the variations in high temperature limits of the model with time [10] and both of these investigations fall under the classification of lumped parameter model.

The thermal analysis tools widely use numerical methods, for example, the finite element method (FEM) and computational fluid dynamics (CFD). Utilizing numerical method analysis can be exceptionally costly as far as model setup and computational time is concerned. Heat conduction problems in solid components can be solved more reliably by using FEM as compared to thermal network. During thermal investigation, the inquiry of heat evacuation and the appropriation of heat sources must also be precisely inspected. In large electrical machines, heat evacuation is guaranteed by thermal convection of air, thermal conduction through the outer frame of the machine and to a less degree by thermal radiation as has been described previously. The general target is to get the learning of the machine's steady state temperatures in the essential design stage. The heat sources that form the input to the thermal equations are taken from the motor losses. The losses in electrical machine comprises of the resistive losses in stator and rotor parts, iron losses in the magnetic circuit, mechanical and frictional losses and additional losses.

Among diverse strategies for thermal investigation of electrical machine, for example, accurate analytical distributed loss model calculation, numerical analysis, lumped-parameter or nodal method, the last one is basic but sufficiently complex to distinguish the temperatures in most areas in the machine.
The electrical machine is separated geometrically into various lumped parts, every part having an interconnection to neighboring segments through contact resistances. It can be assumed in lumped parameter model, that all the generated heat in a specific part represented by a node is assembled to a central point which represents the mean temperature of the section to which the node is placed. The parameters of dynamic LP models are usually extracted from complete dimensional data, the thermal characteristics of the motor utilized and of course the heat exchange coefficients.

2.5.1 Concept of Nodalization

Nodalization is an idea of separating an object into its sub-components, where every component or association point is described by no more than one or possibly a few nodes. The prospect of lumped parameter modeling means the simplified description of the properties of the components in more sensible manner for instance, average temperature at the central point, volume and thermal mass etc. In case a real thing is to be identified with a circuit model involving a set number of parts, a couple of simplifications and assumptions ought to be made.

Nodalization concept can be applied to any particular object in some random way, although there are various factors that should be considered beforehand. Some of these include, are the spots where you need an exact temperature estimate, what the ordinary temperature distribution looks like and the effortlessness in the calculations of the resulting geometry. It can also be in a way that a central point needs to be put at some other spot where the point in itself is not as important,

however, an affiliation is needed between other node points just to increase the accuracy of the model. Considering only the basic geometries first while making calculation of areas and volumes is the key to keep the network simple.

The number of arbitrary nodes can be picked by the model planner, keeping in view the accuracy of the model required, with more nodes mean more detailed information, the price of which is the increased complexity. Provided that the body is somewhat homogeneous making an interpolation between the temperatures of two bordering nodal centers can be a way of achieving acceptable estimation [2].

2.5.2 Placement of Node point in the Geometry [21]

Heat that streams homogeneously from internal to external boundary of any cylinder can be computed utilizing the thermal adaptation of Ohm's law. Two criteria oversee the decision of node location and they are

- Exact forecast of ΔT over the whole surface.
- Exact forecast of the temperature at a particular node point.

In some straightforward objects, for example, a bar which might be considered as thermally detached at both ends, following both the criteria is possible. For a body where thermal resistance and volume per unit length don't change in the same way as the temperature increases, it gets more complicated. Regarding the demonstration of thermal resistance network, making a model with low number of nodes is vital. The inquiry is then- at which radii is it most suitable to infuse the losses, if only one node is to be put in the body and by doing this how big would be the error.

To answer these questions let's begin by characterizing three radii of interest in placing the node point [21]. The resistive midpoint is the point along the heat path through a body where half of the total resistance has passed, and half is left to go. In the case of a hollow cylinder as an example, the equivalent radius is named as $rresMid$ and corresponding node as $nresMid$. The geometrical midpoint is basically the mean of the internal and external radii and is named as $rgeoMid$ and $ngeoMid$. Lastly, the volumetric midpoint is the place where 50% of the item's absolute volume has passed. The comparing parameters are $rvolMid$ and $nvolMid$ [21].

To find out $rresMid$, [21] is utilized to infer a relation to a particular radius where the internal and the external section have the same thermal resistance. The resulting expression is

$$r_{\mathrm{r,M}} = \sqrt{r_{\mathrm{i}} r_{\mathrm{o}}} \tag{31}$$

Where r_{i} is the inner radius and r_{o} is the outer radius. As for $rvolMid$ it is described as

$$r_{\mathrm{V,M}} = \sqrt{\frac{r_{\mathrm{i}}^2 + r_{\mathrm{o}}^2}{2}} \tag{32}$$

The idea of placing the node at $rresMid$ or $rvolMid$ is further illustrated in Figure 5. The tradition in these circumstances appears to be placing the node in the resistive midpoint which is most likely because it is simpler to figure out it that way [21]. However the one which is the most suitable alternative is not evident and will be researched closer for a couple of few relevant cases.

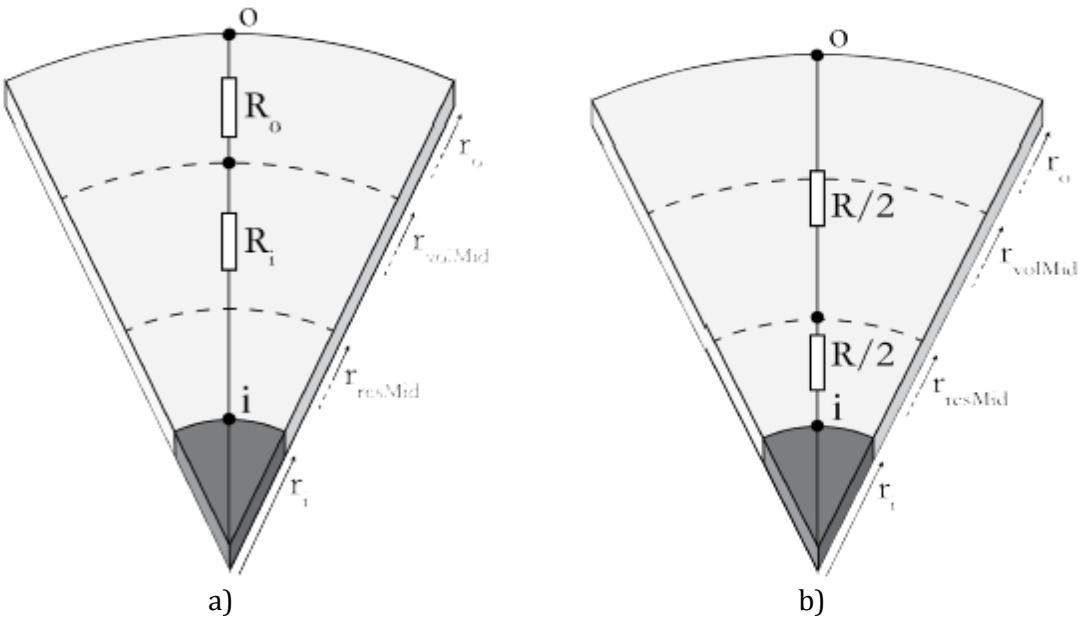

Figure 5: Demonstration of distinction between placing the node at

a) On the volumetric midpoint
b) On the resistive midpoint

2.6 The Controlled Voltage Sources

This section deals with the controlled sources that can be inserted while taking into account the thermal modeling of the machine. As an example the cooling effect can be replaced with a controlled heat source inserted at various node point geometries.

2.6.1 The Effect of Air Flow

Air typically flows with heat exchange. In air space where there are a couple of nodes to be considered, the air stream warms up and moves to an alternate path as losses in the machine. This impact of the air stream can be described by a voltage source between the nodes [11]. Consider the air flow in Figure 6 from the nodes S1, S2, and S3.

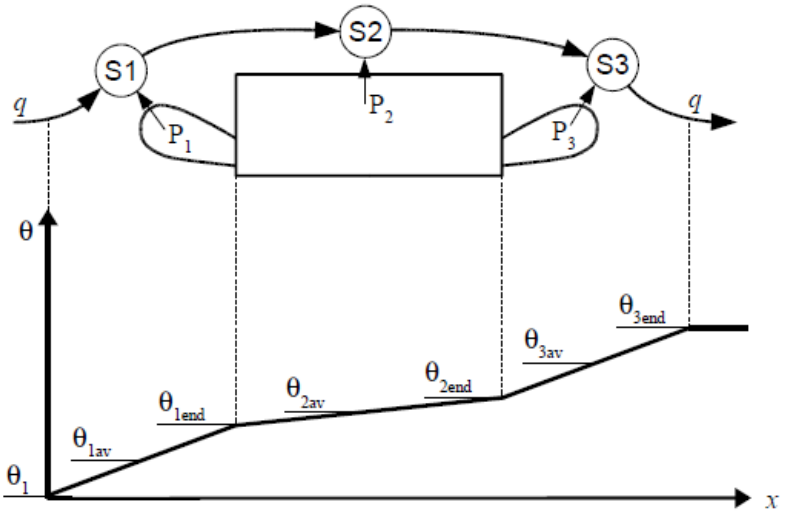

Figure 6: Figure showing the temperature rise at various nodes as air passes through the machine development phase [20]

The above figure can be more generally represented as

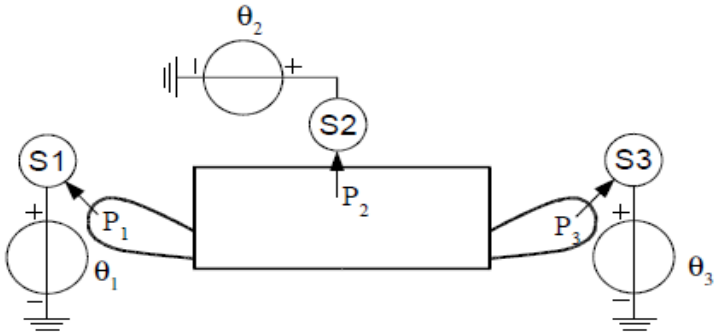

Figure 7: Effect replaced by controlled heat sources ($\theta_1, \theta_2, \theta_3$) inserted at the node points S1, S2 & S3 [20]

Warm ambient air flows to the point S1 and absorbs thermal energy from this node; the future stream of power P_1 of the way. The air is heated from ambient level θ_1 to $\theta_{1,\text{end}}$ wherein the temperature rise of the coil end region is calculated by the equation

$$\theta_{1,\text{end}} = \frac{2P_1}{2\rho c_p q} = 2P_1 R_\text{q} \qquad (40)$$

Where,

$$R_\text{q} = \frac{1}{2\rho c_p q} \qquad (41)$$

Where ρ is the density, c_p is the specific heat at constant pressure, and q is the heat volume flow i.e., the heat flux. In this case it can be assumed to have constant mass flow rate, although the air warms up and expand.

The resistance R_{q} describes the gas flowing ability to absorb heat, in the unit of $(\frac{\mathrm{K}}{\mathrm{W}})$

The average temperature rise of the node S1 is

$$\theta_{1,\mathrm{av}} = \frac{\theta_{1,\mathrm{end}} - \theta_1}{2} = R_{\mathrm{q}} P_1 \qquad (42)$$

Also written as,

$$\frac{\theta_{1,\mathrm{end}}}{2} - 0 = \theta_{1,\mathrm{av}} = R_{\mathrm{q}} P_1 \qquad (43)$$

The same scenario takes place at the node S2, when the air warms up to a point of future power flow P_2 . The average can be specified as

$$\theta_{2,\mathrm{av}} - \theta_{1,\mathrm{end}} = R_{\mathrm{q}} P_2 \qquad (44)$$

When air is heated up to $\theta_{1,\mathrm{end}}$ and flows to a point S2, each node in the thermal stage can be combined to give

$$\theta_{2,\mathrm{end}} = 2R_{\mathrm{q}}(P_1 + P_2) \qquad (45)$$

Node S2 region such as warming up to an average value of $\theta_{2,\mathrm{av}}$ can be specified as the node S1 end temperature and the temperature between the end of the first region and the average of the second region node S2, written as

$$\theta_{2,\mathrm{av}} = 2R_{\mathrm{q}} P_1 + R_{\mathrm{q}} P_2 \qquad (46)$$

The same thing happens at the node S3

$$\theta_{3,\mathrm{av}} = 2R_{\mathrm{q}} P_1 + 2R_{\mathrm{q}} P_2 + R_{\mathrm{q}} P_3 \qquad (47)$$

It can be seen from the Figure 7 that a controlled heat source exists at each node. These sources at various nodes could also be connected between nodes S1 and S2 and between the nodes S2 and S3. $\theta_{2,\mathrm{av}}$ and $\theta_{3,\mathrm{av}}$ can also be written in another form based on the rule 1 [11], which states as

Rule 1: The temperature source connected between a coolant stream node and earth is equivalent to the total of losses assimilated by the coolant before the coolant stream node, multiplied by $2R_{\mathrm{q}}$ and the losses consumed in the coolant stream node increased by R_{q}.

$$\theta_{2,\mathrm{av}} = \theta_{1,\mathrm{av}} + R_{\mathrm{q}} P_1 + R_{\mathrm{q}} P_2 = \theta_{1,\mathrm{av}} + \theta_{12} \qquad (48)$$

$$\theta_{3,\mathrm{av}} = \theta_{2,\mathrm{av}} + R_{\mathrm{q}} P_2 + R_{\mathrm{q}} P_3 = \theta_{2,\mathrm{av}} + \theta_{23} \qquad (49)$$

Where, θ_{12} and θ_{23}can be derived from the voltage source between the nodes as specified in rule 2 [11]

$$\theta_{12} = R_{\mathrm{q}} P_1 + R_{\mathrm{q}} P_2 = R_{\mathrm{q}}(P_1 + P_2) \qquad (50)$$

&

$$\theta_{23} = R_q P_2 + R_q P_3 = R_q(P_2 + P_3) \tag{51}$$

The rule 2 gives the temperature source equations connected between the nodes.

Rule 2: The temperature source between two coolant stream nodes i and j is equivalent to the aggregate of losses consumed by the coolant in the nodes i and j increased by R_q which can verified from Figure 8.

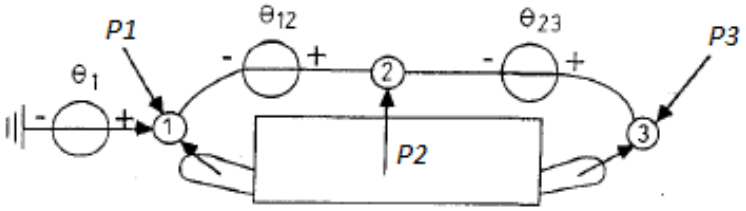

Figure 8: Effect replaced by controlled heat sources ($\theta_1, \theta_2, \theta_3$) inserted at the node points S1, S2 & S3 [11]

2.6.2 The Controlled Voltage-Source Node Point Matrix

When all the conductivity elements are entered in the matrix equation (26), while taking into account all node points, then there can be established relationship between the dependence of conductivity matrix elements and point temperature nodes [11]. These nodes are followed by unknown matrix $[P_u]$ apart from $[P]$ placed on the right side of the equation (29). In this case, the matrix equation (29) is

$$[G][\theta] = \begin{bmatrix} [P] \\ [-P_u] \end{bmatrix} = \begin{bmatrix} [P] \\ [0] \end{bmatrix} - \begin{bmatrix} [0] \\ [P_u] \end{bmatrix} \tag{52}$$

Where $[P]$ is a well-known loss vector, $[P_u]$ is a vector containing injections of loss components (current sources) at various node points and a column vector formed by this is given as

$$[P_u] = \begin{bmatrix} P_{MH2} \\ \cdots \\ P_{MH3} \\ \cdots \\ P_{W2} \\ \cdots \\ P_{W3} \end{bmatrix} \tag{53}$$

MH2 and MH3 are the nodes in the magnetic holder whereas W2 and W3 are the nodes in the windings. Additionally the matrix expressed in (53) can consist of nodes which has unknown future losses, thus the equation (52) cannot be solved without flow of air available.

Let us now take a particular example of the Figure 6. When the air stream flows from the ambient side to the node S1, it is warming up to the warmth of an absorbable average of equations (42), (46) and (47) which can be put in matrix form as

$\theta = G^{-1}P \rightarrow \theta = RP$

$$\begin{bmatrix}\theta_1\\ \theta_2\\ \theta_2\end{bmatrix} = \begin{bmatrix}R_\mathrm{q} & 0 & 0\\ 2R_\mathrm{q} & R_\mathrm{q} & 0\\ 2R_\mathrm{q} & 2R_\mathrm{q} & R_\mathrm{q}\end{bmatrix}\begin{bmatrix}P_1\\ P_2\\ P_3\end{bmatrix} \quad (54)$$

In short,

$$[\theta_\mathrm{u}] = [R_\mathrm{u}][P_\mathrm{u}] \quad (55)$$

Solving the equation above w.r.t $[P_\mathrm{u}]$ and positioning with respect to the equation (52), the heating network in a matrix can be expressed as

$$[G][\theta] = \begin{bmatrix}[P]\\ [-P_\mathrm{u}]\end{bmatrix} = \begin{bmatrix}[P]\\ [0]\end{bmatrix} - \begin{bmatrix}[0]\\ [R_\mathrm{u}]^{-1}[\theta_\mathrm{u}]\end{bmatrix} \quad (56)$$

For this $[\theta_\mathrm{u}] = [\theta]$ moved to the left side, leaving the terms with only the node ratings on the right side we get

$$\left[[G] + \begin{bmatrix}[0] & [0]\\ [0] & [R_\mathrm{u}]^{-1}\end{bmatrix}\right][\theta] = \begin{bmatrix}[P]\\ [0]\end{bmatrix} \quad (57)$$

Which the temperature rise of the matrix $[\theta]$ is solvable as

$$[\theta] = \left\{\left[[G] + \begin{bmatrix}[0] & [0]\\ [0] & [R_\mathrm{u}]^{-1}\end{bmatrix}\right]^{-1}\right\}\begin{bmatrix}[P]\\ [0]\end{bmatrix} \quad (58)$$

2.6.3 Computing of Changed Premises

During this working scenario, thermal behavior is especially irregular to be precise. Demonstrating thermal resistances have been described previously and if capacitances additionally can be, by one means or another, associated with some of the nodes then they must have to be adjusted in the node matrix also. Solving the partial differential equations as

$$[C]\left[\frac{d\theta}{dt}\right] + [G][\theta] = [P] \quad (59)$$

In Matlab ® there is no need to define it in more detail about how the capacitances are taken into account in the calculation. Equations are solved for the first order derivative of $\frac{d\theta}{dt}$ by the help of an aid solver *ode* function incorporated into the final equation. Function *ode* (ordinary differential equation) is a partial differential equation numerical solver, which is based on Runge-Kutta method. However, it should be noted that the capacitances occurs only about half of the node (central point). To solve this allocation there has been made a sub-matrix. Sub matrix equations are

$$\begin{bmatrix}[C_1] & [0]\\ [0] & [0]\end{bmatrix}\begin{bmatrix}[\dot{\theta_1}]\\ [\dot{\theta_2}]\end{bmatrix} + \begin{bmatrix}[G_{11}] & [G_{12}]\\ [G_{21}] & [G_{22}]\end{bmatrix}\begin{bmatrix}[\theta_1]\\ [\theta_2]\end{bmatrix} = \begin{bmatrix}[P_1]\\ [P_2]\end{bmatrix} \quad (60)$$

Matlab ® can be used to describe the first line relating capacitances differential equations and the lower line of ordinary equations.

$$[C_1]\left[\dot{\theta_1}\right] + [G_{11}][\theta_1] + [G_{12}][\theta_2] = [P_1] \quad (61)$$

$$0 + [G_{21}][\theta_1] + [G_{22}][\theta_2] = [P_2]$$

The lower equation can be solved in terms of θ_2 as

$$[\theta_2] = ((-[G_{22}]^{-1}[G_{21}])[\theta_1]) + [G_{22}^{-1}][P_2] \quad (62)$$

When placed it in the upper equation we get a partial differential equation as

$$[C_1]\left[\dot{\theta_1}\right] = [P_1] - [\theta_1]([G_{11}] - [G_{12}][G_{22}]^{-1}[G_{21}]) - [G_{12}][G_{22}]^{-1}[P_2] \quad (63)$$

This can be described briefly as

$$\left[\dot{\theta_1}\right] = A[\theta_1] + B \quad (64)$$

Matlab ® functions *ode*23 and *ode*45 are used to integrate the above sub-matrix equations $[\theta_1]$ in time-stride. This may be followed again by equation (62) to return the values $[\theta_2]$ in time-domain also.

3 The Proposed Thermal Model

In this chapter, network model in terms of thermal resistances has been presented. Starting with the concept of suggested lumped parameter model we end up with simplifications made from geometrical symmetries and suppositions regarding the perfect thermal insulation. Firstly the thermal model of steady state as well as transient state has been presented and then temperature distributions of the models have been solved from thermal machine parts represented by thermal resistances.

Complex machine geometry points to the turbulence model of air stream as it has been examined in the past sections. To counter this, more detailed investigation should be done in comparison with numerical and empirical methods that are generally used for basic geometries. If a complete thermal investigation of high speed machine is to be performed, then the equations should be solved simultaneously in both the solids as well as in fluid domains. One explanation behind this is that the temperature rise in the turbulent fluid and the temperature in the solid parts of the machine intrinsically rely on one another. Actually, the temperature rise of the cooling fluid in a high velocity machine can't be neglected since the coolant removes a lot of heat because of the high loss density [7].

FSPM machine in our case has stator windings and PM's together in the stator region, subsequently, the nearness of the windings and PM's makes a thermal model essential [15].

3.1 Tools

There are numerous methods that can be considered while implementing the geometry of the machine to model thermal network analysis.

3.1.1 3-D Model of Heat Transfer [7]

By presenting a 3-D thermal model of a machine, the temperatures in entire space of the machine can be assessed. The 3D thermal analysis is performed utilizing the COMSOL Multiphysics ® software and is focused around FEM [8].

The domain involving the fluid has been demonstrated in the heat exchange model by defining some outer boundary conditions. The fluid parameters like heat exchange coefficients that have an impact on the thermal behavior of the machine have been mostly taken from existing literatures.

From the above discussion, it can be concluded that the fluid impacts in the 3-D thermal model are presented as conditions on the boundaries in which the solid area has an association with the fluid domain. The outer boundary of the solid material in contact with the cooling fluid can be demonstrated by employing the boundary condition for the heat flux q as

$$-\boldsymbol{n}.q = h(T_{\mathrm{fl}} - T) + q_{\mathrm{o}} \qquad (65)$$

Here h is the heat-transfer coefficient between the solid surface and fluid domain which is taken from existing literature for this sort of machine and T_{fl} is the temperature of the fluid close to the solid surface. The term q_{o} is a general heat flux entering the domain. The boundary condition for thermal insulation of the model is

$$-\boldsymbol{n}.q = 0 \tag{66}$$

The above mentioned condition is mostly utilized for demonstrating the boundary condition on which the solid surface domain is insulated. This limit condition is likewise utilized for reducing of the model size by exploiting the symmetry as will be carried out in our situation to be described in the upcoming section of the thesis.

An alternate limit condition that is utilized is to consider constant ambient temperature at the boundary given as

$$T = T_{\mathrm{o}} \tag{67}$$

This condition is for demonstrating a boundary on which the temperature T_{o} is known in advance. The boundary condition that describes the heat generated between two solid surfaces is given as

$$-\boldsymbol{n}_{\mathrm{up}}.\left(q_{\mathrm{up}} - q_{\mathrm{dw}}\right) = q_{\mathrm{o}} \tag{68}$$

Here q_{o} is the generated heat flux on the surface i.e., the heat flux entering the domain. This mathematical statement expresses that the difference of the normal component of heat fluxes on the upper and lower side of the problem domain are equivalent to the heat flux generated on the surface. The eddy current losses are mostly described with the heat source q_{o} . If there is no heat generation between two solid surfaces then q_{o} = 0.

3.2 Suggested Lumped Parameter Thermal Simulation Model

To make the thermal simulation model to work, it can be broadly divided into three parts

- Structuring the thermal model for the machine
- Evaluating the thermal resistances
- Calculating the losses from the electromagnetic model and their location in the machine

In the model developed for evaluation of thermal phenomena, the object under investigation is partitioned into a few thermal components represented by node arrangements, the elements of which are then linked together to form complete thermal model comprising of nodes and resistances [9], [17].

The thermal system is like an electrical system which has current sources as losses infused at different node points. The temperature of the ambient air is usually taken as a reference value θ_{a} (T_{a}).

Simulation can also be made for the transient analysis and is based on the following differential formula as has already been mentioned in (59) [9]

$$\frac{d}{dt}(\Delta\theta) = C^{-1}\left(\Delta P - G(\Delta\theta)\right) \tag{69}$$

Where ΔP is the loss vector containing the losses dissipated to a specific node and $\Delta\theta$ is the temperature rise vector as given in (27) and (28) respectively and G is the conductance matrix already defined in (26).

It must be recognized that when cooling of electric machines are investigated; a cooling matrix must be utilized to get dependable results. This is on the grounds that the vast majority of the created hotness is expelled from the inner parts of the machine with the help of fluid flowing through the machine. Thus a cooling conductance matrix has to be defined for this purpose and the temperature distributions in the machine can be evaluated by (70). In an unlikely event when the cooling matrix is ignored, conduction becomes the main source of heat exchange which ultimately can lead to wrong temperature distribution [18].

$$\theta = (G + G_{\mathrm{fl}})^{-1} P \qquad (70)$$

It is vital to consider both the electromagnetic as well as the thermal models when it is desired to get reliable results because of strong collaboration between the two i.e., losses subject to temperature rise and vice versa (see Figure 9). Especially sensitive to temperature change are parts which are in the vicinity of the air, as thermal properties of air are strongly dependent on the temperature.

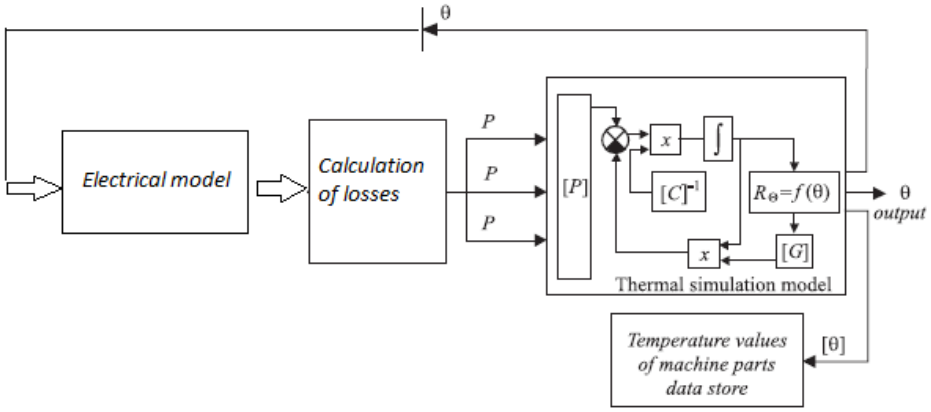

Figure 9: Block diagram of simulation model consisting of electrical and thermal model [9]

3.2.1 Distribution of Power Losses and their occurrence [12]

A suitable thermal investigation requires faultless assessment of the losses and their occurrence inside the machine. For low and medium speed machines, copper losses contribute to the major part of the total losses which can be obtained systematically by the estimation of stator winding resistance and stator current mostly by experimentation. Since the copper losses depend on the temperature, the careful measurement of the losses can iteratively be computed with the temperature adjustment.

The iron losses mostly occur in the stator yoke and teeth. The eddy current losses occur mostly in permanent magnets and rotor disk, which for low speed applications can be neglected but for high velocity machines it has to be incorporated in the thermal model. [13] gives some methods to determine the eddy current losses in PM's and also in the rotor disks lying in the region of permanent magnets.

The losses obtained in this way must be inserted at various node points in the LP model. The losses also occur internal to the motor classified as electrical, mechanical and frictional losses with former

depends on the temperature distribution and the latter two on the rotational speed of the machine [18]. The resistances of the stator windings are temperature dependent like the resistive losses and there are two ways to take this temperature dependency into account in loss calculations. In the first option, the numerical solution of the coupled field circuit equations gives the losses in the windings by the evaluation of phase resistance with operational temperature. This can give accurate results, but since the stator windings are usually at lower temperatures as compared to coil end windings, the losses in the end windings can somehow be underestimated. Another alternative can be to calculate the losses of the stator windings iteratively in the actual thermal analysis [18].

In COMSOL the heat sources in the windings have been declared by the loss P_{L} as

$$P_{\mathrm{L}} = \frac{|J|^2}{\sigma_{\mathrm{Cu}}} \tag{71}$$

Where J is the current density and σ_{Cu} is the electrical conductivity of copper. Since this thesis is only concerned about the thermal modeling so the loss calculations and their origin in the machine has not been considered in depth.

3.3 Steady State TEC Model of FSPM Machine

3.3.1 Objective

Our main objective is to create a TEC model (thermal equivalent circuit) for an axial flux switching permanent magnet machine. For this reason we will construct electrical elements (resistances, current sources and capacitances) analogue to the discretized thermal elements (thermal resistances, heat power sources and thermal capacitances) and will estimate all of them. Finally we will solve the circuit to know the temperatures and heat fluxes in the motor.

3.3.2 Main Geometry of the Motor

A typical three dimensional illustration of a dual rotor axial flux switching permanent magnet machine with 10 rotor poles and 12 stator poles is shown in Figure 10 [34]. As a comparison with conventional radial PM machines, an axial PM machine has advantages associated with it in the form of shorter axial length, improved efficiency and better heat dissipation. FSPM machines on the other hand have experienced a rapid growth in popularity owing to their high power density and torque capability [34]. The FSPM motor, investigated in this report consists of 6 stator poles and 7 rotor poles. Due to the low number of stator and rotor poles and their geometry, the machine can be represented in some convenient shapes (see Figure 13). As for the structure of flux switching permanent magnet machine where the rotor consists of only iron, it can be presumed that no heat actually flows through the rotor structure [33].

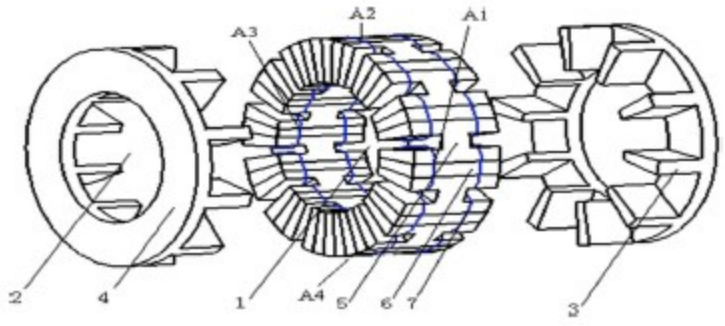

Figure 10: Three dimensional illustration of axial FSPM with 10 rotor and 12 stator poles [34]

Topology includes 1) stator 2) Rotor 3) Rotor pole 4) Rotor yoke

5) Stator core 6) Permanent magnet 7) Winding

As the stator of the machine under investigation in this thesis has 6^{th} order symmetry around the main (z) axis (not exactly the rotor, as it is rotating), we will exploit this symmetry for our purpose. The same symmetry will also be valid for the temperatures and the heat fluxes. A typical thermal equivalent system of the FSPM motor considering the entire section and the machine parameters is shown in Figure 11. By utilizing all the machine specifications, as depicted in Figure 11, the thermal resistances (see Figure 13) and capacitance values (see Figure 14) of various motor elements can be obtained.

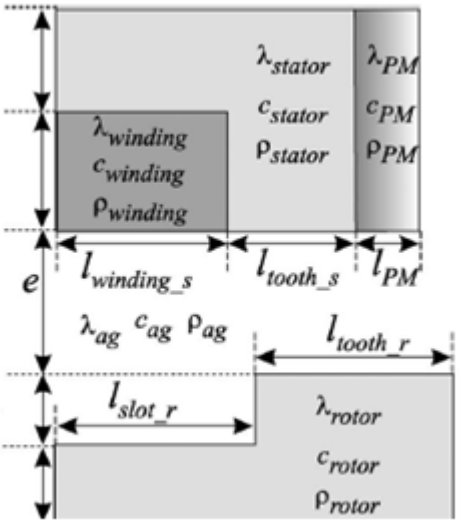

Figure 11: Machine parameters of the equivalent thermal system of a typical FSPM motor [33]

Where $l_{windings\_s}$ is the length of primary stator slot whereas $\lambda_{winding}, \rho_{winding}$ *and* $c_{winding}$ are the equivalent thermal conductivity, density and specific heat capacity of the primary stator slot respectively.

By assuming z-axis to be vertical, the machine under investigation has still two more symmetries: one is around a horizontal plane (to which main (z) axis is normal and in the middle of the motor), and the other is around the vertical plane which divides the stator in two equal halves. After taking into account all these symmetries, we have $1/24^{th}$ specific elementary cell of the geometry.

The final geometry cell ($1/24^{th}$ sector of the whole machine), is the one in which we will define and will estimate the resistances for the thermal model in steady state case and also the capacitances in the transient state case. Note that the radial/axial heat flux for each tooth of the whole motor will be two times the flux we will compute model with this reduced version, but the temperatures will be the same as the computed ones. Of course, this is because that the resistances of the tooth will be reduced by the same factors.

3.3.3 Heat Generated (in PM) from Induction (by Windings)

As we know, a current carrying conductor when placed in a magnetic field experiences a force. Same scenario which will occur is that currents will be induced in an electrically conductive body when it will be placed in magnetic field varying with time, which ultimately would result in thermal power generation on the surface of the body. This phenomenon, which is typically used in industries, is referred to as induction heating. To produce time varying magnetic field we must have some proper arrangement of conductors and the source must also be adjusted accordingly to provide time varying current in the induction coil. Thus the electrical energy provided to the induction coil gets converted into thermal power without any physical connection through the process of induction heating and electromagnetic phenomena. Practically the power sources used in this process involve alternating current supplied to the induction coil, the frequency of whose varies from application to application.

The current intensity induced by this way is most critical at the surface of the object under investigation but decays as we move away from the surface towards the center considering the limits of thickness/skin depth ratio. As this ratio increases, more and more lost power is scattered near the surface, a phenomena known as skin depth (δ).

Thermal power and induction heat efficiency produced in the induction coil or any particular object under investigation can be found for general shapes, for instance, round and empty bars or tubes, cylinders and wide rectangular pieces etc., by the use of some already built empirical and semi empirical formulas in existing publications. The only drawback that comes with numerical and analytical methods of existing publications is that they assume material properties to be constant, while in reality electrical resistivity (ρ_{r}) and specific heat capacity are among the few variables which are temperature dependent whereas few parameters like permeability of materials (μ) are dependent both on the magnetic field strength and temperature.

For general solid circular segment resembling square or rectangle with fillets of diameter d and length L, heated in some encasing having N turns with a current of I A/turn wound around the coil of diameter D and length L_{c} , the induced power P_{W} is approximately given by [21], [23], [24] as

$$P_{\mathrm{W}} = (NIK_{\mathrm{c}})^2 \frac{\pi d\rho}{\delta L} Q_{\mathrm{rod}} \qquad (72)$$

Q_{rod} in this expression is an empirical constant which is given in Figure 12 as a function of d/δ and K_{c} is also an empirical constant which is dependent on the ratios of d/D, d/δ and L/L_{c} .

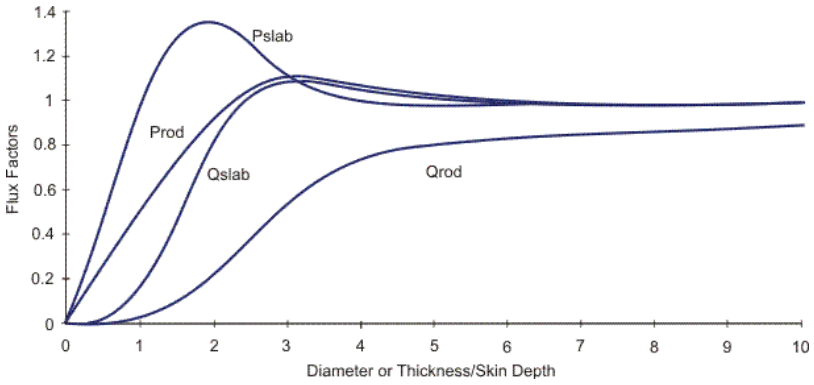

Figure 12: Flux factors Q and P for rods and slabs [25]

The TEC model used in this report is based on the following assumptions [13], [14], [15], [18]

- The nodes taken for temperatures are representative of the entire piece to which they are associated.
- When heat power is generated inside a piece, it can be assigned to a central node point.
- Heat flux is mainly radial in rotor tooth.
- Heat flux is mainly axial in the stator.
- Air flow between stator and rotor i.e., in the air gap is laminar and convection phenomena between their faces are proposed to be equal to the static surfaces with constant areas (i. e. , rotation effect is included in Nusselt number).
- All far temperatures for convection fluxes can be taken just as an ambient temperature.
- The convective coefficients for all horizontal faces are the same, independent of their size, position (faces are 'just' horizontal) or other nearby components. For instance, we neglect the difference between convective coefficients of parts with different velocities.
- The former point applies for all vertical faces as well.
- Rotation has been taken into account just inside convective coefficients, so they should be high enough (much higher than in the static case).
- All convection heat fluxes to far air follows the simple Newton's law (i. e. , h is constant).
- Permanent magnets are assumed to have a uniform temperature inside.
- All the symmetries (transversal plane, vertical plane and $1/6^{th}$ turn − rotation) apply for all temperatures and fluxes, thus only a $1/24^{th}$ part of the motor has been analyzed.
- In transient case, capacitances are assigned to a central node point inside the corresponding piece.
- Contact resistances between elements are neglected.
- Radiation phenomenon is neglected.

3.3.4 Resistances, Dimensions and Circuit for Steady State Analysis

Table 2 below gives the dimensions, resistances and losses inserted at a particular elementary cell of the geometry analysed ($1/24^{th}$ part of the machine) with Figure 13 gives the steady state TEC model of FSPM machine under consideration.

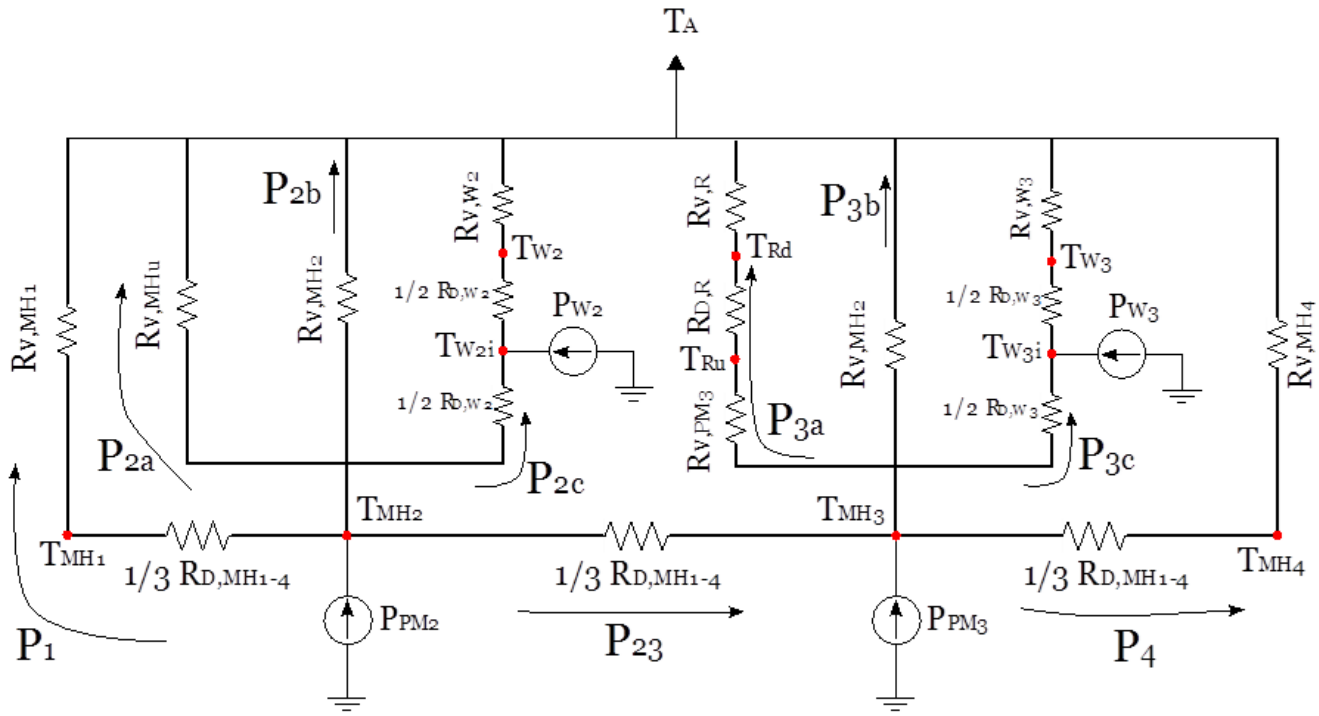

Figure 13: Steady State TEC Model of Flux switching PM machine

Table 2: Description of Dimensions, Resistances and Losses inserted

Resistances of the elementary cell $\left(\frac{1}{24}^{th}\ part\right)$	
RD_MH1_4	Main conduction resistance in MH (axial direction)
RD_R	Conduction resistance (axial direction) in rotor
RD_W2	Conduction resistance in winding 2
RD_W3	Conduction resistance in winding 3
RV_MH1	Convective resistance from face 1 of MH to open air
RV_MH2	Convective resistance from face 6 of MH to open air
RV_MH4	Convective resistance from face 2 of MH to open air
RV_MHu	Convective resistance from upper face of MH to open air
RV_PM3	Convective resistance between stator and rotor

RV_R	Convective resistance from upper face of rotor to open air
RV_W2	Convective resistance from face of winding 2 to open air
RV_W3	Convective resistance from face of winding 3 to open air
Losses inserted at the elementary cell $\left(\frac{1}{24}^{th}\ part\right)$	
P_PM2	Heat power in PM2, due to induction, in W
P_PM3	Heat power in PM3, due to induction, in W
P_W2	Heat power in W2, due to Joule losses, in W
P_W3	Heat power in W3, due to Joule losses, in W

The model in figure 13 has been built keeping in view one elementary cell of the geometry and assuming modeling techniques that have already been discussed in section 2.5 with few exceptions regarding the heat flows in the analysis.

Table 3 nicely describes the parameters of the TEC model of FSPM machine given in the Figure 13.

Table 3: Parameters of TEC Model

Region	**Parameter**	**Heat Transfer mechanism**	**Losses inserted at node points**
Magnetic Holder	$R_{\mathrm{D,MH1-4}}$	Conduction	$T_{\mathrm{MH2}} \sim P_{\mathrm{PM2}}$
Magnetic Holder	$R_{\mathrm{V,MH1}}$, $R_{\mathrm{V,MH2}}$ $R_{\mathrm{V,MH4}}$	Convection (vertical faces)	$T_{\mathrm{MH3}} \sim P_{\mathrm{PM3}}$
Magnetic Holder	$R_{\mathrm{V,MHu}}$	Convection (horizontal faces)	-
Windings	$R_{\mathrm{D,W2}}$, $R_{\mathrm{D,W3}}$	Conduction	$T_{\mathrm{W2i}} \sim P_{\mathrm{W2}}$
Windings	$R_{\mathrm{V,W2}}$, $R_{\mathrm{V,W3}}$	Convection	$T_{\mathrm{W3i}} \sim P_{\mathrm{W3}}$

Rotor	$R_{D,R}$	Conduction	-
Rotor	$R_{V,R}$	Convection	-
Air-gap	$R_{V,PM3}$	Convection	-

3.4 Transient State TEC Model of FSPM Machine

In problems which are time dependent, thermal energy stored in a system is represented as thermal capacitances [1]. Some nodes are assigned with thermal capacitances from that particular node to the ambient. The thermal capacitance of a particular element or part is usually obtained from material properties and geometrical data available.

3.4.1 Circuit for Transient State Analysis

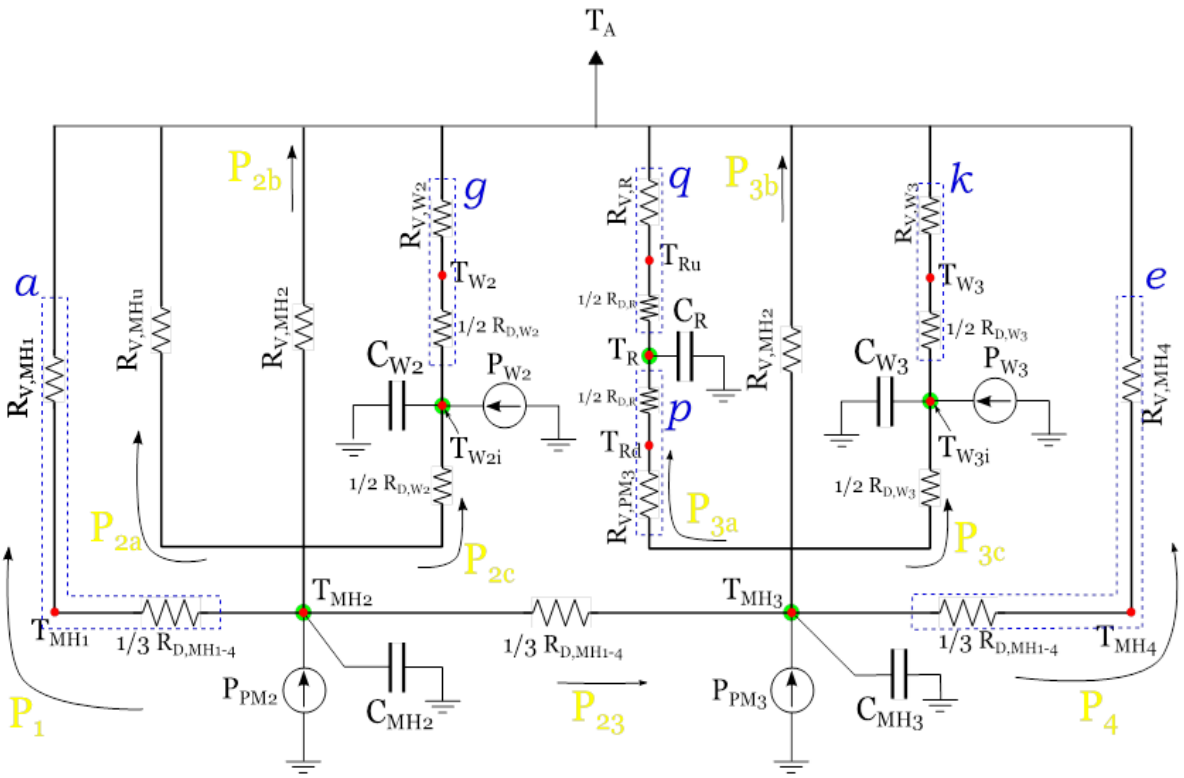

Figure 14: Transient State TEC Model of Flux switching PM machine

The main five knots of the transient state circuit shown in Figure 14 are represented by green-red dots to which capacitances have been added.

3.4.2 Heat Capacity and Electrical Analogue

A heated body when cooled drops its temperature or changes its state. As we don't consider here any change of phase, we will consider only temperature increase.

The relation between the heat absorbed by the body (Q) and the increment in temperature (θ) at constant pressure is given here as in (15)

$$Q = m\, c_p\, \theta \tag{73}$$

By dividing both sides of last equation by the elapsed time, we get the relationship between the heat power source and the ratio of temperature increase as

$$P = m\, c_p\, \frac{\Delta\theta}{\Delta t} = m\, c_p\, \dot{\theta} \tag{74}$$

For a (electrical) capacitor we have the following expression

$$Q = C\, \mathrm{V} \tag{75}$$

Where Q is the electric charge stored, C is the capacitance and V is the capacitor voltage.

Taking derivative w.r.t time

$$I = C\, \dot{\mathrm{V}} \tag{76}$$

Thus the thermal analogue of the electrical capacitance is: mc_p

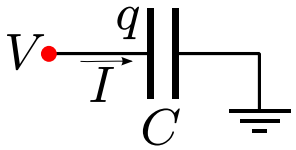

Finally, a good electrical model for a solid body could be the following one given in Figure 15.

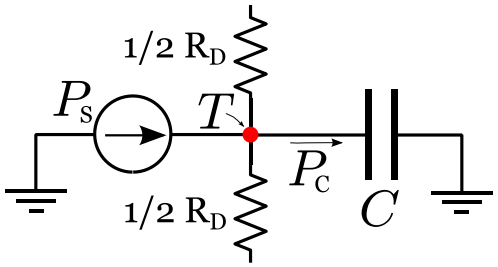

Figure 15: Electrical Model for a solid body

Where P_S is possible heat power source inside the body (generally due to Joule's effect), C is the thermal capacity of the body, R_D is the conductive resistance (there would be others, if heat conduction takes place in other directions) and T is a representative of inner temperature of the body.

3.5 FEM-Simulation

The settings done while implementing the FEM-simulations follow the rules which have been described in the scope of this thesis with couple of few special cases. Some comments on how they were realized in COMSOL are as follows

- The coolant was simulated by setting a constant steady temperature of the external boundary.

- The temperatures utilized when comparing the FEM-simulation results with the thermal network models were obtained by taking the temperatures of a central point of the nodes placed at nearly the same location on the system, the actual node point would correspond to.

- To decrease the simulation time the study module was run only for “heat transfer in solids (ht)”, “heat transfer in liquids” and for “laminar flow”.

- The mesh was refined to the degree that further refinement did not fundamentally change the reenactment of results.

- The simulation of windings was assumed by considering a domain to be defined over the stator bars and permanent magnets. The thermal conductivity of the materials was also declared for both the sectors as in the thermal resistance network.

- In COMSOL Multiphysics model, air was considered as solid by defining an outer box boundary. It doesn't however handle the way that the air was always moving and generally homogenous in its temperature distribution. As it doesn’t, it implies that hardly any heat will flow in the segment of the air gap and ΔT over the air gap will hence not be reliable and to be precise will somewhat be overestimated.

3.6 Computational Procedure

The computer program for the thermal analysis of FSPM machine is written by using Matlab ®. Figure 16 represents the flow chart of the program for the FSPM electrical machine. The input parameters are the dimensions, physical parameters and cooling methods of the machine. Based on the input data, the coefficients of heat exchange and losses are determined. After this, thermal resistive components are calculated and solved for temperature distribution. The final output of the computation is the temperature rise distribution of the machine as a function of flow rate and heat transfer. Additionally the flow rate between various node points can also be specified.

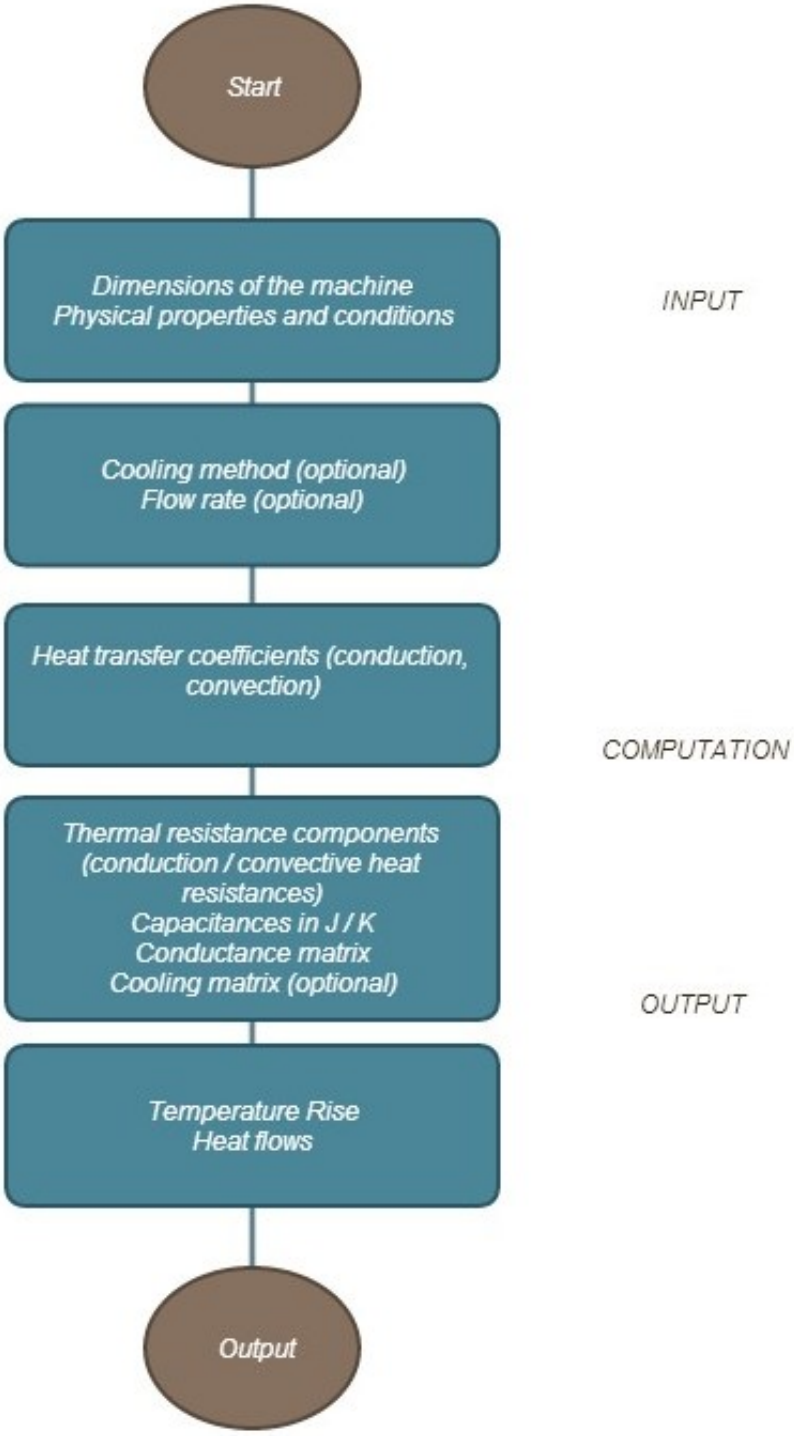

Figure 16: Flow chart for the computation of temperature rise in FSPM electrical machine

4 Structural Optimization

Structural optimization in the field of electromechanics is a combination of several nomenclatures. Optimization in a broader term is referred to as to "making things the best". Consequently, structural optimization is a subject of gathering of materials, plans and actions identified with machine geometry in the most idealized way. The task in this section of the thesis is to find a machine structure that is most optimal to work out with. Clearly such optimizations i.e., maximizations and minimizations can't be performed without any starting lower bound and upper bound indicated. For example, if there is no limit on the number of winding turns, the length of the PM's and different parameters that have a close relationship with the optimization algorithms, then we have an unbound optimization problem which don't have a well-defined result.

Constraints in structural optimizations are mostly linked with the geometry of the machine. Most quantities that are treated as constraints can be used in the optimization algorithms as an objective function. Thus the designer can check the performance criteria of the design structurally by checking the imposed limits, and then the structural optimization can be achieved by having an objective function that needs to be optimized i.e., maximized or minimized by using few or more parameters that directly affect the efficiency of the machine.

- Objective function (f): An objective function is a function that can be used to classify designs. For every particular design, f shows the decency of the design. Usually f is chosen such that a small value i.e., minimization is better than a large one. In our particular scenario f measures the losses which are to be minimized by genetic algorithm or simulated annealing (to be described later in this section) to improve the overall efficiency. It is also named as fitness function in some standard optimization algorithms.

- Design variable (x): A vector of parameters that portrays the design employed, and which can be made variable during optimization. It may represent geometrical dimensions or physical quantities.

- State variable (y): A function or vector that represents the response of the structure for a given design x.

A general structural optimization (SO) problem takes the form [29] as,

$$(\text{SO}) \quad \begin{cases} \text{minimize f(x, y)with respect to x and y} \\ \{\text{subject to} \begin{cases} \text{behavioral constraints such as lower bounds and Upper Bounds} \\ \text{initial values as in simulated annealing} \end{cases} \end{cases}$$

4.1 Global Optimization

Global optimization uses that sort of strategies that allows the designer to discriminate between global optimum point and several local optimum points in a specific area under investigation. Global optimization problem generally follows unconstrained optimization.

Conventional global optimization methods can generally be classified into two types which are

1. Deterministic methods
2. Stochastic methods

An outline of the design in which efficiency is most elevated is not generally the best plan as there can be numerous angles to be considered in motor design procedure including simple assembling, reliability, dependability etc. Generally discovering an acceptable approach to consider all these parameters into a single objective function is extremely troublesome, so a powerful multi-objective optimization algorithm is needed.

There are indeed issues to develop multi-objective optimal configuration for a particular machine. The first and foremost reason is that all geometrical constraints such as lower bounds, upper bounds and behavioral considerations can't be considered. Additionally, the time-consuming analyzes such as transient temperature rise analysis cannot be performed in the course of optimization process because of time cost.

We, in this manner, utilize just the most relevant parameters in building an objective function and in applying strategies [29] that distinguish different variables by locating local as well as global optima. That is to say, the planner can utilize numerous criteria and his experiences to select the best design among generated solutions.

Two particular algorithms employed in this thesis are

- Genetic Algorithm (ga)
- Simulated Annealing

While general optimization algorithms have the capacity to converge to the highest one and discard others, genetic algorithms and simulated annealing can identify multiple optimal profiles.

4.2 Genetic Algorithm (ga)

Genetic Algorithm is among the methodology of Artificial Intelligence that uses a computer to simulate the nature's process of development and selection. Genetic Algorithms are used to solve the issues which are ill-behaved, discontinuous and non-differentiable [31]. Since the rise of genetic algorithms was in the late 1970s, global optimization has been one of the real targets and tons of exertions have been dedicated to create effective algorithmic models to handle global optimization issues. Simulated Annealing is one of the effective models among these.

4.2.1 Working Procedure of Genetic Algorithms

As has already been mentioned that, genetic algorithmic calculations are focused around the methodology of natural selection, they take the essential properties of natural selection and apply them to any issue under consideration. The basic process for a genetic algorithm includes following steps

1. **Initialization** - Create a random initial population (array of individuals) [30]. This population is normally arbitrarily produced and could be any size, from just a couple of individuals to thousands. 'PopulationSize' tags how many numbers of individuals there are

in each generation. With a huge 'PopulationSize', the genetic algorithm looks for the result space more thoroughly, consequently lessening the risk that the calculation will return neighborhood minima that is not global minima.

2. **Evaluation** - Each individual of the population is then assessed to ascertain a fitness value for this individual in the generation. The fitness value is computed by how well it fits with outlined prerequisites.

3. **Selection** – There is always a need to continually improve population's fitness function value. Selection helps to do this via disposing the bad designs with the help of few selection methods and just keeping the best individuals among the generations in the population. Some individuals, named as elite individuals [30], in the current generation that have best fitness value to minimize the losses are selected for next generation automatically.

4. **Crossover** - During crossover we create new individuals by combining the properties of our chosen individuals.

5. **Mutation** - We need to add a little bit randomness into our populations' genetics else each blend of results we make would be in our introductory population. Mutation typically works by introducing little improvements to parents.

6. **And repeat!** - Now we have our next generation of individuals, we can start again from step 2 till we have an end condition.

The genetic algorithm over and again adjusts a population of individuals. At each one stage, the genetic algorithm chooses parents from existing individuals in the generation and uses them to produce children by crossover and mutation processes in the next generation until an optimal solution is found. The algorithm stops when stopping criteria (stall generations) is met, which is the point at which the normal relative change in the fitness function value over stall generations is short of tolerance function value, whose default quality is 1E-06 [30].

The genetic algorithm differs from traditional optimization algorithm in two main ways, as summarized in the following Table 4.

Table 4: Difference between Traditional Algorithm and Genetic Algorithm

Classical Algorithm	**Genetic Algorithm**
A single point is created during each single iteration, with a succession of points created during iterations that approaches an optimal result.	Generates a population of points at each iteration. The point having the best fitness function value approaches an ideal or optimal result.
Chooses the next point in the sequence of events by deterministic computation.	By using random number generators, selects the next population of individuals.

The flow diagram of the Genetic algorithm (ga) is described in Figure 17 as

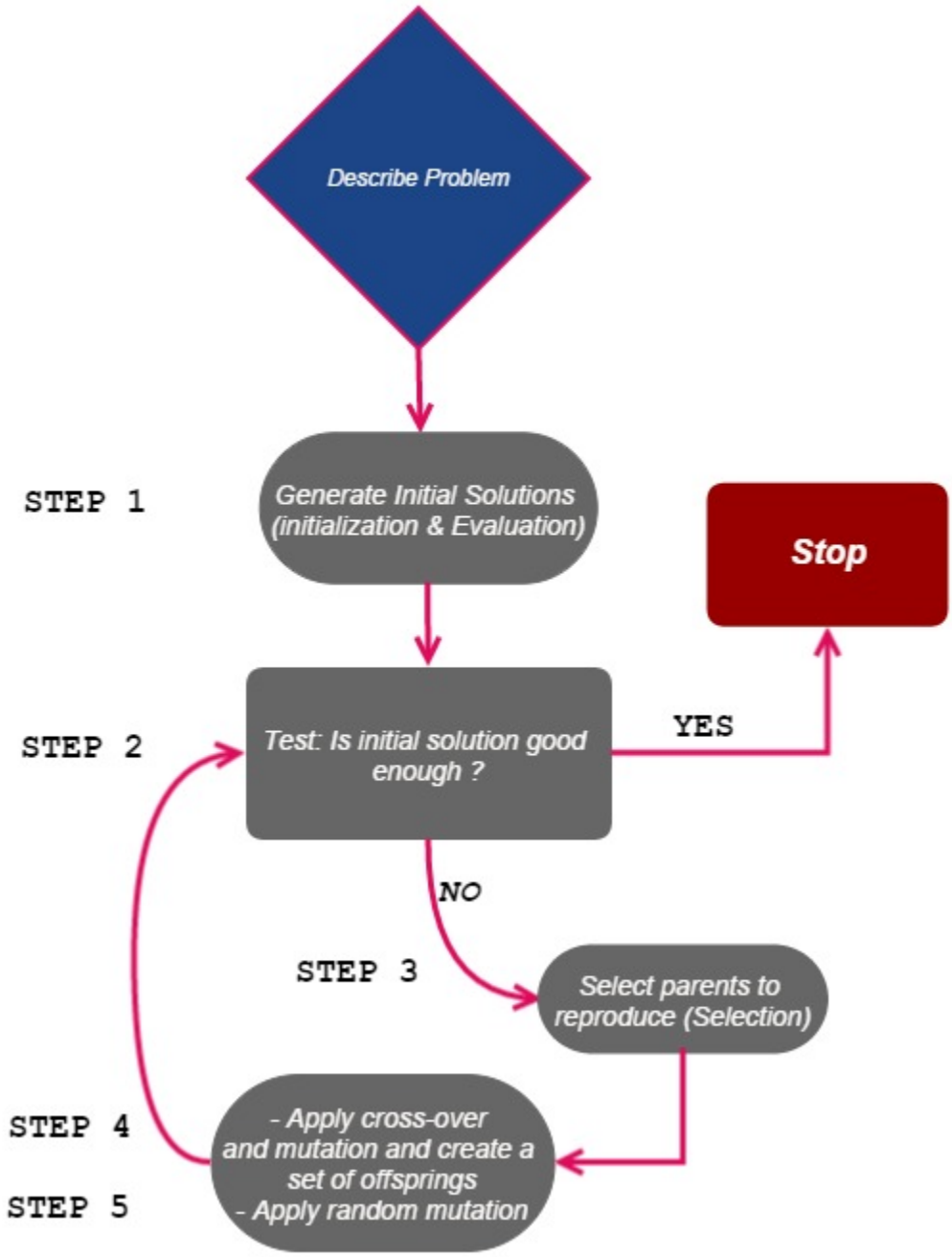

Figure 17: Flow diagram of Genetic Algorithm

4.3 Simulated Annealing

For streamlining issues of optimization, finding some optimal result can be at times very troublesome. This is on the grounds that when an issue gets sufficiently extensive we have to look for a large number of acceptable answers to find which one best suits our problem. Indeed with the present day processing power of computers there can still be excess of possible answers to consider. In this situation where we can't sensibly hope to discover an optimal result in a reasonable length of time, what we can do is to settle for something that is close enough i.e., one of the local optima.

To discover a good enough result in a sensible span of time we have to utilize such a calculation algorithm that is able to do so. It has already been defined in the previous section that such a problem can be solved by the use of genetic algorithm. Additionally there are other less difficult calculation strategies that we can use to get nearly ideal results. In this section the algorithm concept introduced is simulated annealing.

The algorithm of simulated annealing is motivated from the concept of metal piece annealing which includes warming and cooling a piece of metal or any material to change its physical characteristic because of progressions in its inside structure. In simulated annealing, heating methodology is employed by considering a temperature variable. We at first set it high and afterwards permit it to gradually cool as the calculation proceeds. As long as the temperature parameter is reasonably high enough the algorithm will be permitted with more recurrence, to acknowledge results that have worse values as compared with the present values. This gives the algorithm a capacity to bounce out from any nearby local point. The likelihood of acceptance of higher values of objective function i.e., the worse solution points as compared to the current one is reduced as the temperature is reduced. This permits the calculation to steadily concentrate on the inquiry space in which there is a chance to find close to a global optimum result.

4.3.1 Working Procedure of Simulated Annealing

Simulated annealing is a strategy for explaining the optimization issues which are either unconstrained or bound constrained. The basic steps [31] are

1. First and foremost there is a need to set the 'initial temperature' and make an arbitrary starting result (initial values).

2. At that point it starts to decrease the temperature until termination criteria is met. Normally it is such that either the framework has cooled enough, or a sufficient result has been obtained.

3. Next step is the selection of neighboring point by making little improvement to our current result.

4. If the neighboring point yield result that is better as compared to the current point solution, shift to that point otherwise not.

5. Lastly, decrease the temperature and follow the same procedure.

Each iteration creates a new point haphazardly. The distance between the two points or the in depth search through the space to find a global optimum is based on the probability distribution function. The calculation algorithm acknowledges all new points that bring down the value of the fitness function in case of minimization problem. Additionally, with certain likelihood, also acknowledges the points that raise the value of objective function in an attempt to move out of any local minima. The probability of acceptance is [31]

$$\frac{1}{1+\exp\left(\frac{\Delta}{\max(T)}\right)} \tag{77}$$

Where,

$\Delta=$ new objective function value $-$ old objective function value

$T =$ Temperature at the instant of iteration

An annealing timetable is chosen to deliberately lower the temperature as the calculation continues. As the temperature gets lower, the calculation algorithm decreases the degree of its search to find an optimal result in the search space. The algorithm stops when stopping criteria is met [31].

The flow diagram of the Simulated Annealing algorithm is described in figure 18 as

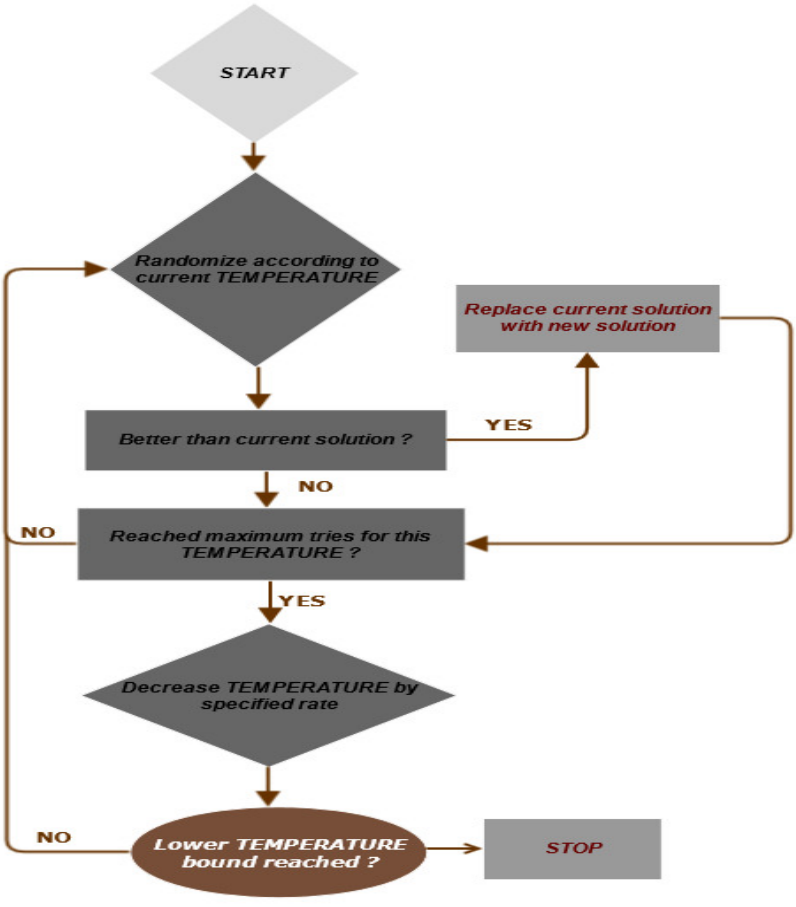

Figure 18: Flow diagram of Simulated Annealing

5 Results

The results presented here are all based on investigations on steady state as well as on transient analysis, implying that the purpose of operation has stayed steady long enough for all the parameters and temperatures to reach to their final operating states. Furthermore, the ambient temperature is assumed to have a constant value of $T_{\mathrm{amb}} = 40°\mathrm{C}$. For some particular application where cooling phenomena of different parts of the machine is not that constructive, the temperature increase beyond ambient in the simulation would be higher, and thus there would be less border line before maximum thermal limits.

The results presented here are both from the solutions of network analysis as well as from FEM simulations and care should be taken while making a comparison between the two. The network analysis gives the nodal temperatures which normally mean the temperature of the central node or body. The FEM simulation on the other hand, furnishes us with the precise value of temperature at any specific point in the concerned machine. As the differences between the two mentioned strategies are not very large, the results presented should also display less arbitrariness. Having the capacity to see compliance of results between the thermal resistance network model and the FEM model, the latter gives useful evidence towards the reliability of results.

The steady state simulation of the machine is done with the solution methods presented in Section 3. The results are produced for the machine when it is simulated with all parameters set to their typical values. The idea behind this is to check the results obtained from the thermal resistance network modeling considering nodalization, in terms of quality of the network developed. Table 5 contains the output from the steady state and transient analysis and presents how well the FEM and the network solutions agree. The highest discrepancy between measurements and finite element analysis occurs in the magnetic holder (horizontal) which is about 19 °C followed by the magnetic holder (vertical) about 12 °C with all other component temperature differences less than 10%. The network results are higher compared to those obtained using finite element analysis, and the reason would probably be the assumptions for the end regions and the effect of convective heat transfer in the finite element model. In the lumped parameter model, however, axial heat flow was also considered for better agreement of the results.

Investigations between the lumped parameter and finite element analysis demonstrate that in all parts of the machine the lumped parameter model yields higher temperatures. Possible reasons for this are the consideration of convective resistances to ambient in the lumped network since this will result in an increase in the temperature. Moreover, in addition to convective coefficients to be same for all vertical faces and also same for all horizontal faces, the thermal conductivity in the axial direction was taken to be exact as that in the radial direction since the FEM analysis does not permit the details of anisotropic thermal conductivities [23].

Table 5: Comparison of the simulation results from thermal resistance network model and the FEM-simulation

Nodes		FEM [°C]	Thermal Resistance Network	
			Steady State Temperature	Transient Temperature
			T[°C]	
Magnetic Holder	T_{MH1} $(vertical\ face)$	$T_{\mathrm{MH}}Vertical$ 105.0948 °C	117.473 °C	$T_{\mathrm{MH}}Vertical$ 117.8235 °C
	T_{MH4} $(vertical\ face)$		117.053 °C	
	T_{MH3} $(vertical\ face)$	$T_{\mathrm{MH}}Horizontal$ 98.8491 °C	119.397 °C	$T_{\mathrm{MH}}Horizontal$ 119.3973 °C
	T_{MH2} $(horizontal\ face)$		117.823 °C	
Windings	T_{W2}	T_{W2i} 126.4224 °C	115.027 °C	T_{W2i} 129.8179 °C
	T_{W2i} $(Inner\ windings)$		129.818 °C	
	T_{W3}	T_{W3i} 131.4463 °C	116.440 °C	T_{W3i} 132.0164 °C
	T_{W3i} $(Inner\ windings)$		132.016 °C	
Rotor	T_{R}	T_{R} 40 °C	66.380 °C	T_{R} 66.3799 °C
	T_{Ru} $(tip\ of\ the\ rotor\ disc\ facing\ ambient)$		66.337 °C	
	T_{Rd} $(tip\ of\ rotor\ facing\ airgap)$		66.423 °C	

To talk about the expressions for heat power inside the windings and PM's, it can be assumed that each winding has a heat source caused by Joule's law (heat generation due to current and electrical resistance of the body: ohm's law) as

$$P_{\mathrm{W2}} = \frac{N_2 L_{\mathrm{WT2}} I_2^2}{\sigma_{\mathrm{W}} S_{\mathrm{W}}} \tag{78}$$

$$P_{\mathrm{W3}} = \frac{N_3 L_{\mathrm{WT3}} I_3^2}{\sigma_{\mathrm{W}} S_{\mathrm{W}}} \tag{79}$$

Also permanent magnets are affected by the varying magnetic field produced by the windings. The result is the eddy currents, which also yield heat by Joule's law. The expressions for the heat powers induced in the PM's are

$$P_{\mathrm{PM2}} = \frac{K_c^2 Q_{\mathrm{rod}} I_2^2 \sqrt{8\pi\, S_{\mathrm{PM2}}}}{2\sigma_{\mathrm{iron}} \delta\, L_{\mathrm{PM1}}} \tag{80}$$

$$P_{\mathrm{PM3}} = \frac{K_c^2 Q_{\mathrm{rod}} I_3^2 \sqrt{8\pi\, S_{\mathrm{PM3}}}}{2\sigma_{\mathrm{iron}} \delta\, L_{\mathrm{PM1}}} \tag{81}$$

K_{c} and Q_{rod} are empirical constants which depend on the coil as well as on the core of the geometry. In the Matlab ® code developed, product of $K_{\mathrm{c}}^2 Q_{\mathrm{rod}}$ have been taken as 0.25 but in actual scenario, this value should be estimated by experimentation as given in Figure 12.

Table 6 gives the values of losses used to obtain the temperatures of Table 5 by considering the formulas (78) – (81) and using the defined values of the variables.

Table 6: Values of losses inserted at various node points

Heat Power Sources (W)	Description	Value
P_{PM2}	Heat power in PM2, due to induction in W	6.2822 W
P_{PM3}	Heat power in PM3, due to induction in W	5.8759 W
P_{W2}	Heat power in W2, due to Joule's losses in W	0.1200 W
P_{W3}	Heat power in W3, due to Joule's losses in W	0.1248 W

By applying Kirchhoff's law to the five knots ($T_{\mathrm{MH2}}, T_{\mathrm{MH3}}, T_{\mathrm{W2i}}, T_{\mathrm{W3i}}, T_{\mathrm{R}}$) of Figure 14, we come up with loss vector having the terms defined as

$$P = [P_{\mathrm{PM2}} + \frac{T_{\mathrm{amb}}}{R_1} \; ; \; P_{\mathrm{PM3}} + \frac{T_{\mathrm{amb}}}{R_2} \; ; \; P_{\mathrm{W2}} + \frac{T_{\mathrm{amb}}}{g} \; ; \; P_{\mathrm{W3}} + \frac{T_{\mathrm{amb}}}{\mathrm{k}} \; ; \; \frac{T_{\mathrm{amb}}}{q}] \tag{82}$$

Where,

$$a \equiv R_{\mathrm{V,MH1}} + \frac{R_{\mathrm{D,MH1\text{-}4}}}{3}$$

$$e \equiv R_{\mathrm{V,MH4}} + \frac{R_{\mathrm{D,MH1\text{-}4}}}{3}$$

$$R_1 = a \parallel R_{\mathrm{V,MHu}} \parallel R_{\mathrm{V,MH2}} \tag{83}$$

$$R_2 = R_{\mathrm{V,MH2}} \parallel e \tag{84}$$

$$g = R_{\mathrm{V,W2}} + \frac{1}{2} R_{\mathrm{D,W2}} \tag{85}$$

$$\mathrm{k} = R_{\mathrm{V,W3}} + \frac{1}{2} R_{\mathrm{D,W3}} \tag{86}$$

$$q = R_{\mathrm{V,R}} + \frac{1}{2} R_{\mathrm{D,R}} \tag{87}$$

5.1 Calculation Results

The thermal resistance network is obtained by the method described in Section 3 for steady state and also for transient state. For steady-state analysis the temperature rise vector is obtained by (30). The temperature of 40 ℃ is chosen as a reference ambient temperature. The calculated temperatures of the different parts of the machine for steady state and transient analysis are presented in the Table 5 with the values of losses given in Table 6. The temperatures for transient state are obtained by writing equations for the transient circuit described in section 3.4 including the effect of thermal capacitances. Figure 19 shows the calculated nodal temperatures in transient state at normal operating point of the machine with ambient temperature of 40 ℃.

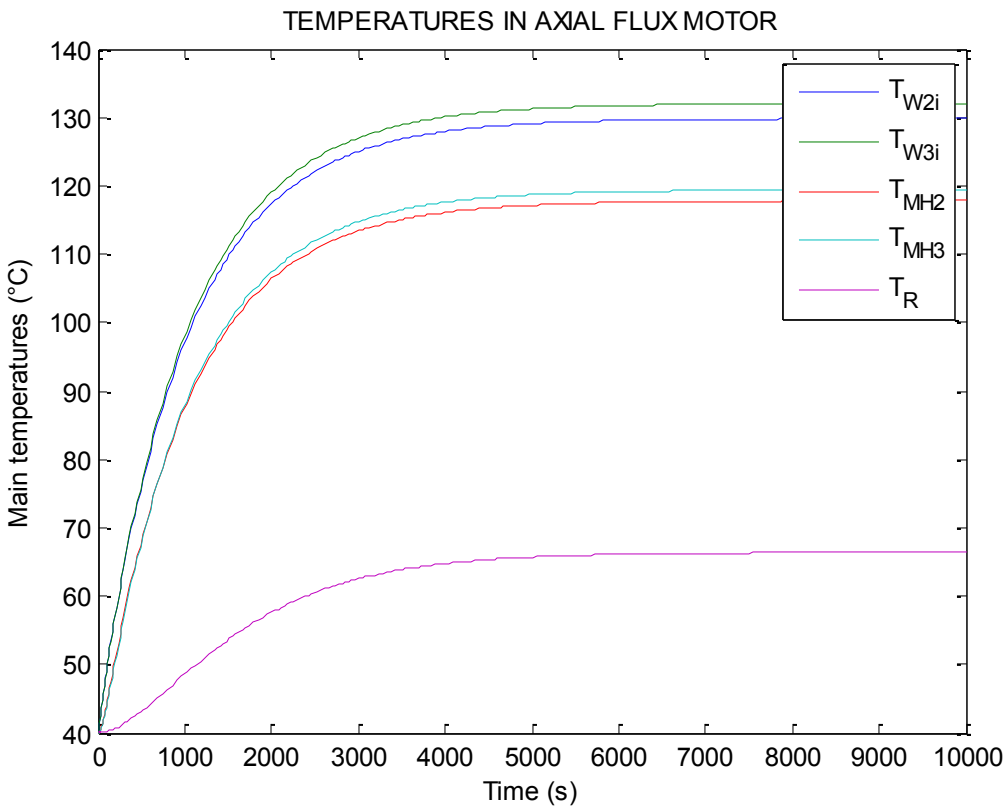

Figure 19: Temperatures in various parts of FSPM motor in transient state

As it is evident from Figure 19 that approximately one hour is required for the heat transfer i.e., the temperature rise to reach its steady state. Thermal failure in FSPM machine is known to occur in the stator (windings) as this is in fact the most heated region.

One important concept here is that it is not only the magnitude or the uncertainty of resistances that matters, their placement in the thermal design of the motor can also be of even greater significance. Since windings of the machine are considered as a source of heat (losses), the winding losses and the other additional losses in the machine are eventually very important to the temperature rise and are highly dependent on the loading. High speed as an example increases the windage and iron losses, while the copper losses are proportional to torque. What is more important is perhaps the estimation of the total temperature increase in the body. In order to see the absolute temperature of various parts of the machine, Figure 20 gives us a nice overview. Here W2 is the name given to windings 2 corresponding to PM2 and W3 for windings 3 corresponding to PM3.

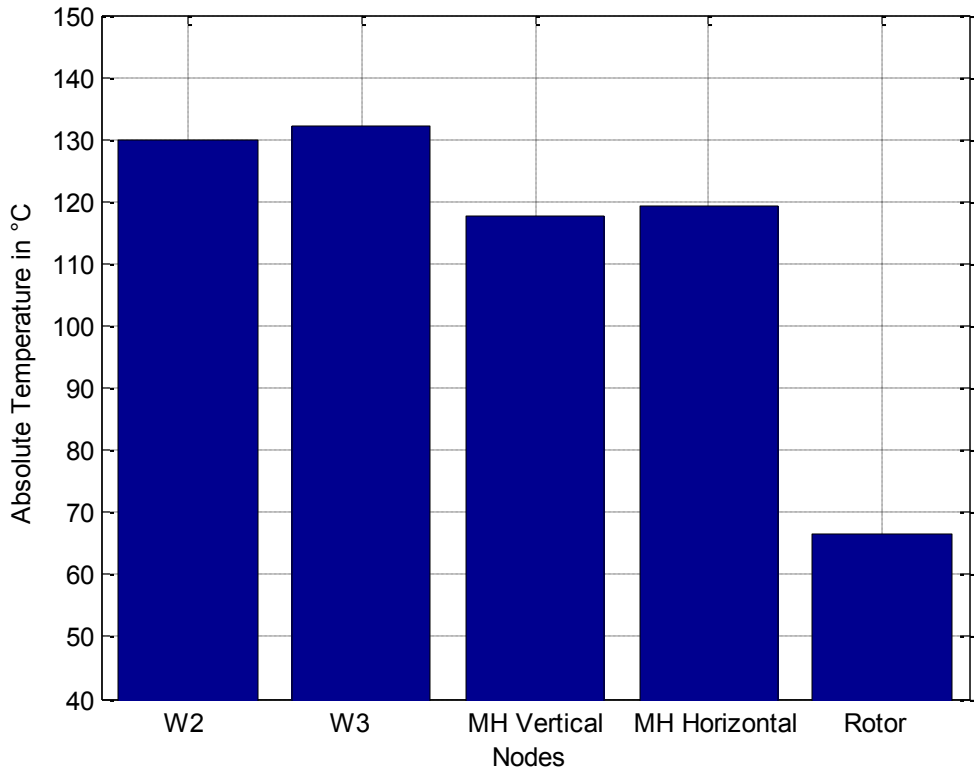

Figure 20: Absolute Temperature of various machine parts

Apart from this fact that FEM-results are possibly more reliable and accurate in some sense, they are in a few ways subject to the same instabilities and inaccuracies in the data information about the machine as the network system model itself. An example would be an error in the estimation of the interface gap between two materials which would result in the same error for both the models. But when simulation of the air gap is concerned, the network system model is presumably more dependable and gives reliable results, as it handles the flow of air better than the FEM.

Looking at the nodes in Figure 21, it can be seen that the network temperatures are higher as compared to the FEM solution. This can be justified that if a thermal network model is properly developed, then it will give the average temperature rise of a certain part when total losses of that part are inserted at that point, whereas in FEM it will give exact temperature at that particular point of interest, which is not the average temperature and hence there might be some overestimation in the developed thermal equivalent circuit.

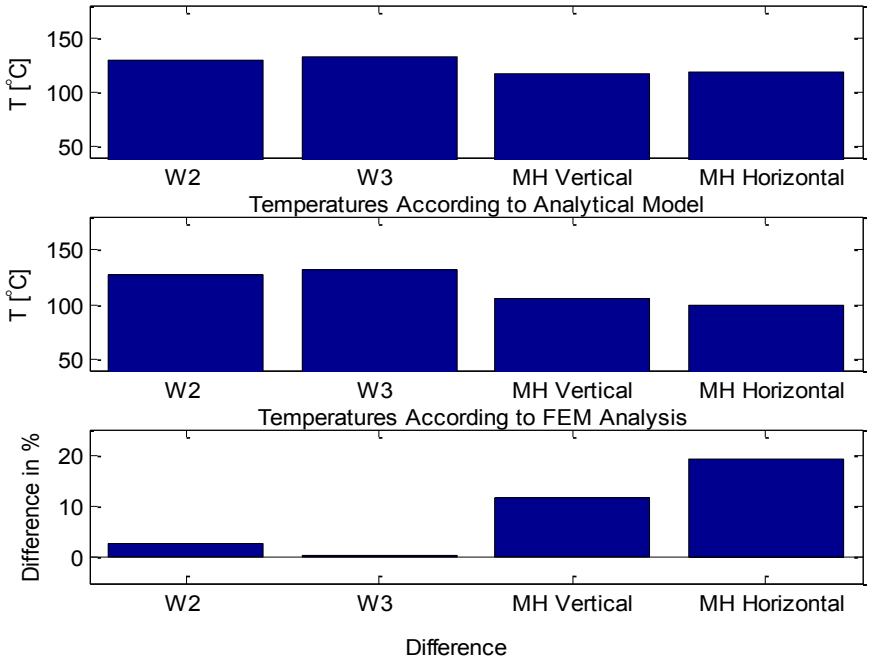

Figure 21: Comparison between the Analytical model and the FEM Analysis

The magnetic holder's (vertical and horizontal) node temperature does not agree well between the models and there is somewhat large difference between the two. This can be expected from the overestimation of the shape of the magnetic holder. Additionally the heat transfer would have been improved if it was actually all surrounded by iron rather than some air, which is the case with our current geometrical shape.

5.2 Sensitivity Analysis

In order to check how the errors in the parameters of the developed thermal model affect the temperature predictions a sensitivity analysis was performed. The sensitivity of the developed thermal model to evaluate the correctness of the various thermal coefficients of different parts of the machine under investigation was evaluated by changing the convection coefficients by 20% from what was previously used in calculating the temperature of various parts. Equally it is evident from Figure 22 and Figure 23 that changing the convective heat transfer coefficients have significant effects on the calculated nodal temperatures. When the convection heat transfer coefficients are increased by 20% (+20%) the nodal temperatures have decreased approximately by 11% whereas when the coefficients are decreased by 20% (−20%) the nodal temperatures have increased by approximately 14%. The convective resistance between the rotor and the stator (air gap) has some influence on the temperature, especially on the rotor temperature as permanent magnets are linked to rotor disc surface via the air gap. Larger air gap will eventually increase the cross sectional area of the permanent magnets that would result in larger heat accumulation across the permanent magnets lowering the convective resistance. Since the heat is dissipated through this resistance this ultimately would result in lower heat dissipation across the rotor disc and hence increase in rotor temperature.

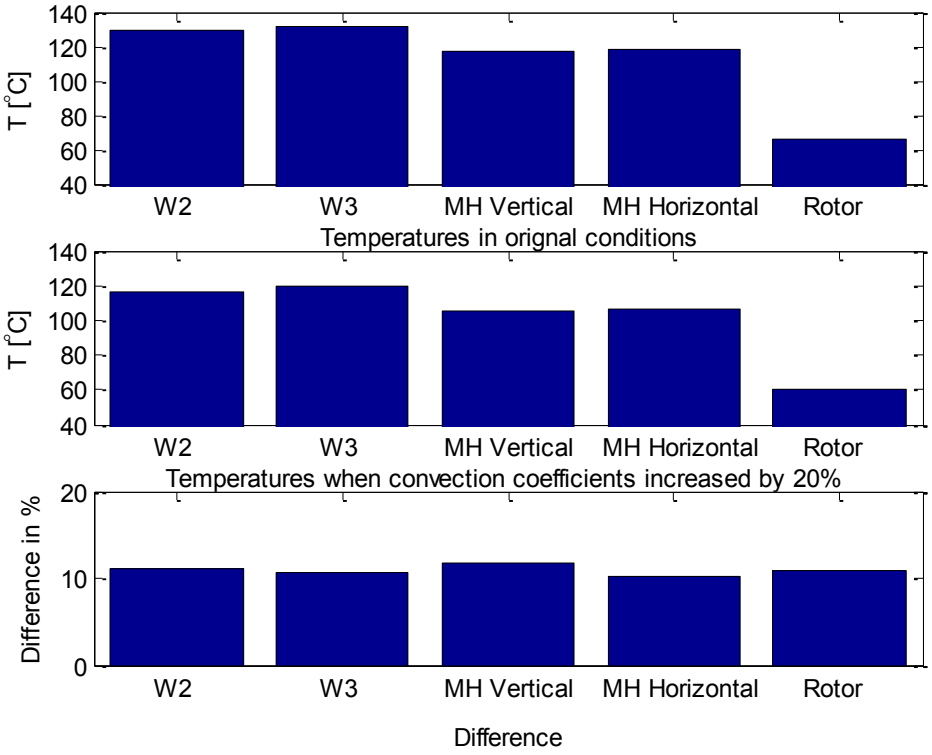

Figure 22: Comparison of calculated temperatures with nominal heat transfer coefficients and when coefficients are increased by 20%

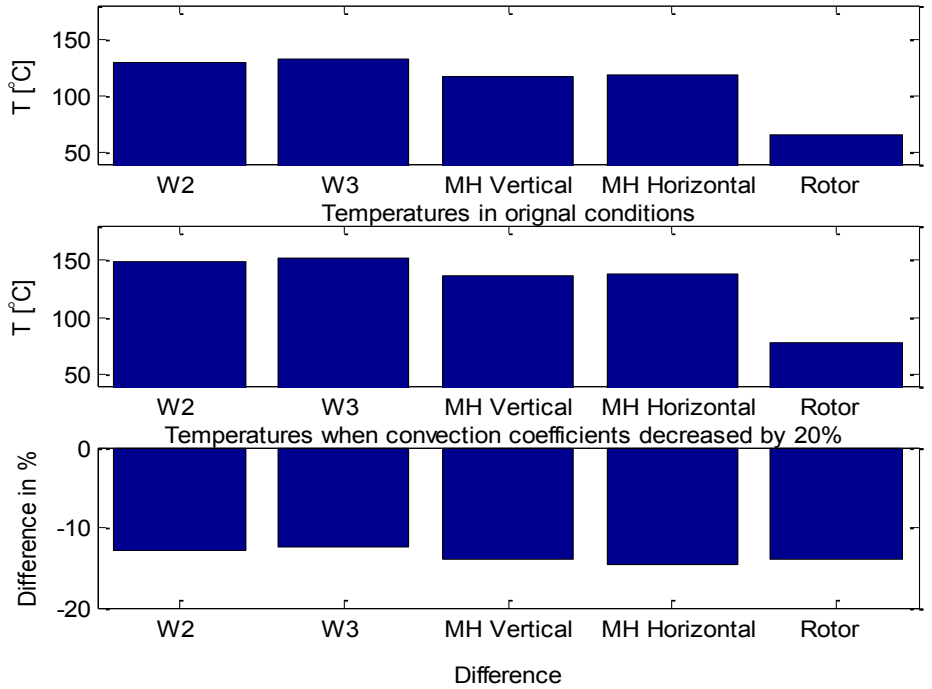

Figure 23: Comparison of calculated temperatures with nominal heat transfer coefficients and when coefficients are decreased by 20%

The surface area of permanent magnets has an effect on the resistance. In order to check the influence of cross sectional area of the permanent magnets on the nodal temperatures, consider the effect when surface areas of permanent magnets have changed by 30%. When the cross sectional areas of the permanent magnets have increased by 30% (+30%) the nodal temperatures have increased approximately by 6% and rotor by 11% and when decreased by 30% the nodal temperatures have decreased by 10% and for rotor by 15% as depicted in Figure 24 and Figure 25.

The correct estimation of motor losses is of even greater importance in the thermal network model. To have a glimpse of this we have changed the losses defined by Joule's law for permanent magnets and also for the windings by $\pm 50\%$. When the losses have increased by 50% then the temperature of the nodes have roughly increased by 40% whereas decreasing the losses by 50% have decreased the temperature of the nodes by 50% as shown in Figure 26 and 29.

The variations of thermal conductivities and the dimensions have only a minor effect on the temperature prediction.

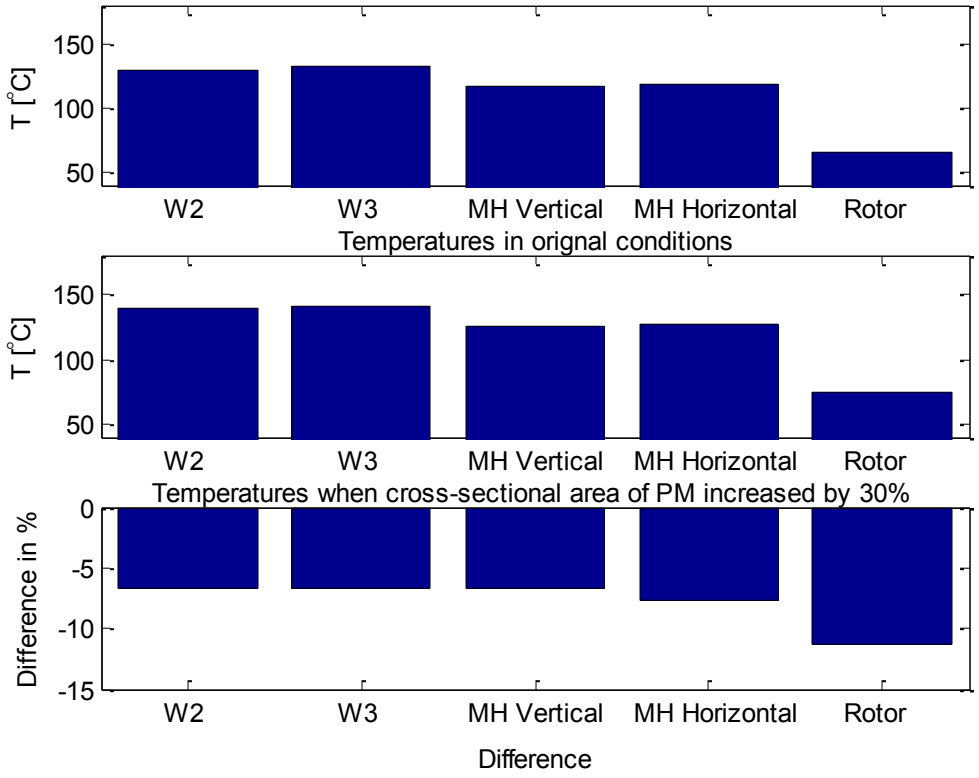

Figure 24: Comparison of calculated temperatures with surface area of permanent magnets increased by 30%

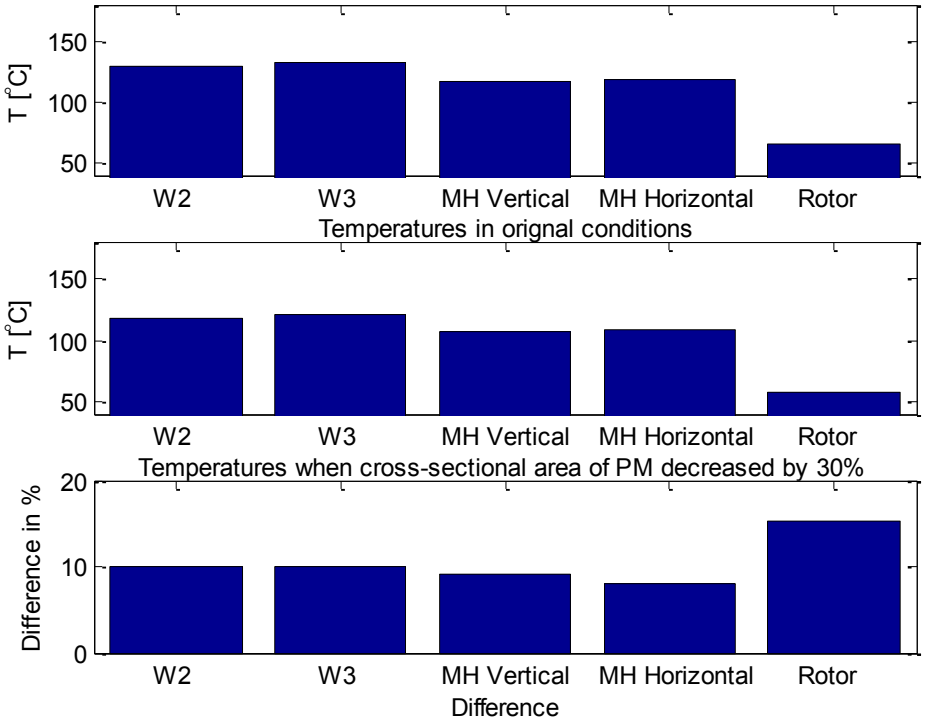

Figure 25: Comparison of calculated temperatures with surface area of permanent magnets decreased by 30%

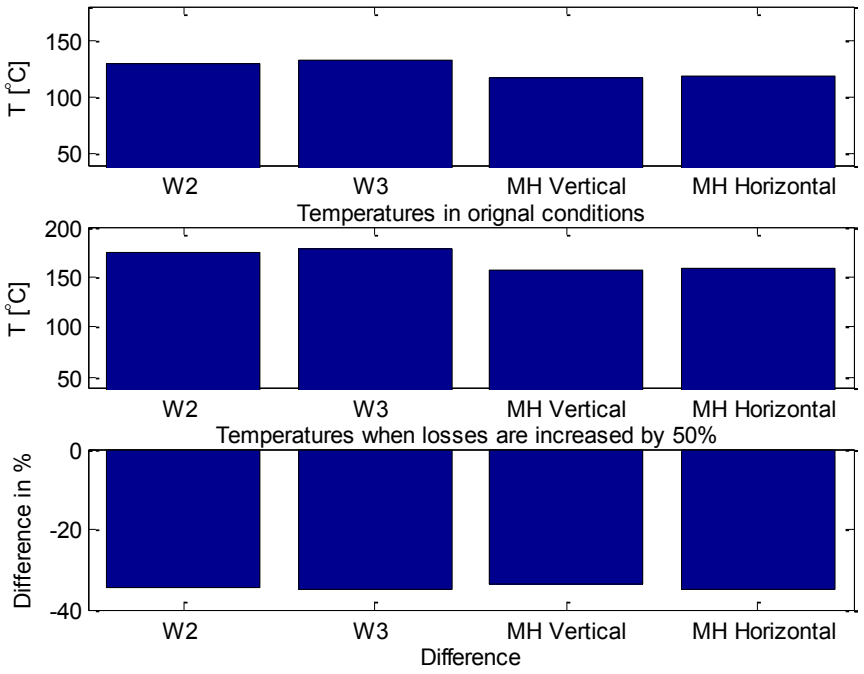

Figure 26: Comparison of calculated temperatures with the nominal losses and when losses increased by 50%

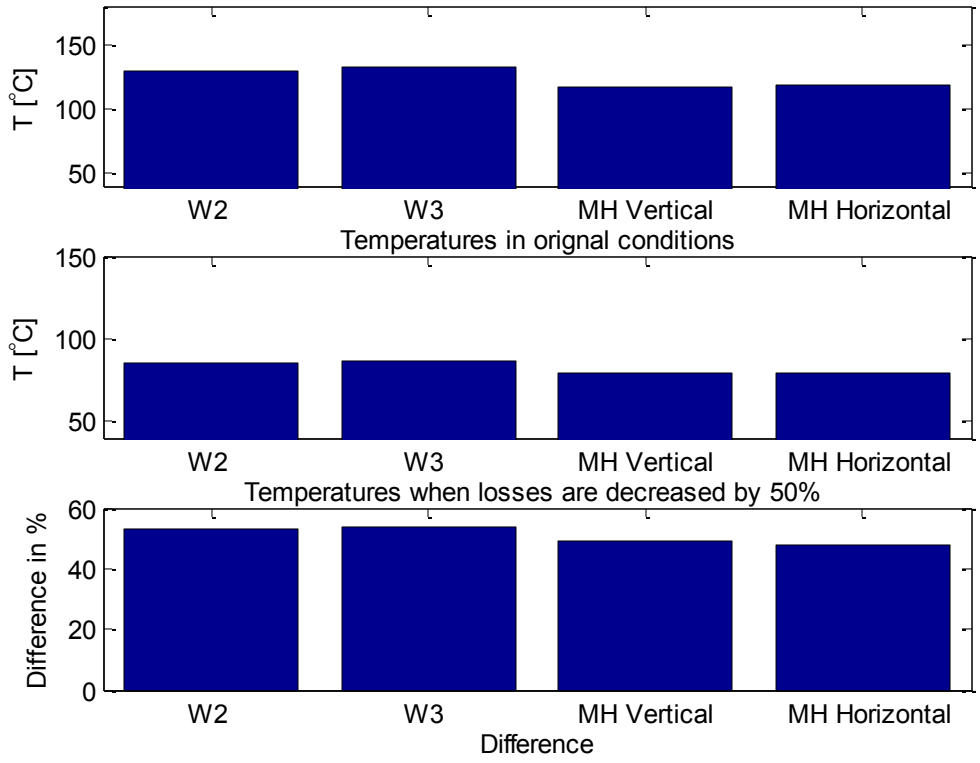

Figure 27: Comparison of calculated temperatures with the nominal losses and when losses decreased by 50%

To talk about the validation of the modeling results by measured results it can be concluded that, for sensitivity analysis to be performed a number of parameters have been chosen and swept. The results show that the model developed has some nonlinearities and uncertainties because the input data is either uncertain or the network developed has low resolution. An example could be interface gap and its coefficients which may differ greatly between individual machines and is mostly evaluated by the electromagnetic demands of the designer. The model has assumed a laminar flow however turbulence phenomena might be among the more uncertain aspects of the design, for which reason the nodal temperatures in various parts of the machine are not certain to be precise.

5.3 Optimization Results

After properly defining the minimization problem of optimization, few initial simulations were run to check whether the generated results are reliable and valid and that the yield gives what sort of output in light of in-feasible sets of configuration variables, bounded and unbounded constraints and defects in the lower limits and upper limits. Experience has demonstrated that this is vital keeping in view the fact that it happens frequently that as the designer tries to fluctuate the estimated values of the outline variables, the configuration model does not remain valid. Under such circumstances we can get the results by just changing the limits or by modifying configuration variables as some percentage of other parameters in the design constraints.
After the establishment of valid setup for investigation, the accuracy of the optimization has been increased by using non-linear constrained analysis with constraints on temperature of the

permanent magnets and the windings and by using finer lower and upper bounds. Two optimization algorithms have been employed to optimize the machine, so that results can be compared. These two methods as discussed previously are genetic algorithm and simulated annealing respectively.

Genetic Algorithm (ga) and Simulated Annealing allow constraints in the input vector (here the input vector is the six variable fitness function, whose elements are all dimension and the non-linear constraints that have been added globally as the temperature of permanent magnets and windings. Non-linear constrained optimization can only be done for genetic algorithm as simulated annealing allows only bounding the vector of parameters.

The machine program code for the structural optimization of the machine is composed in Matlab ®. Figure 28 represents the flow chart of the program for an electrical machine.

If we want to have constraints on torque also, a good estimation of power produced (mechanical) and power consumed (electrical) can only be obtained from complete electromechanical study. As the model under consideration is only thermal, real power and torque cannot be computed from it alone.

The results from two optimizations are summarized below. The quantity of inspections or iterations needed to achieve the ideal configuration i.e., optimal result can likewise be seen by using display commands in the algorithms used for optimization calculations in light of the fact that it is an essential measure of the efficiency of the optimization processes. To achieve the design goals, an objective function has been created, the sensitivity of whose depends on the six input arguments (variables) selected. The arguments chosen to optimize the dissipated losses are:

L_W8	$\%\ Height\ of\ windings, in\ m.$
$N2$	$\%\ Number\ of\ turns\ of\ winding\ 2.$
$N3$	$\%\ Number\ of\ turns\ of\ winding\ 3.$
S_PM2	$\%\ Cross\ section\ area\ of\ (half)\ section\ of\ narrow\ PM, in\ m^2.$
S_PM3	$\%\ Cross\ section\ area\ of\ (half)\ section\ of\ wide\ PM, in\ m^2.$
S_MHu	$\%\ Horizontal\ upper\ area\ of\ (half)\ section\ of\ MH, in\ m^2.$

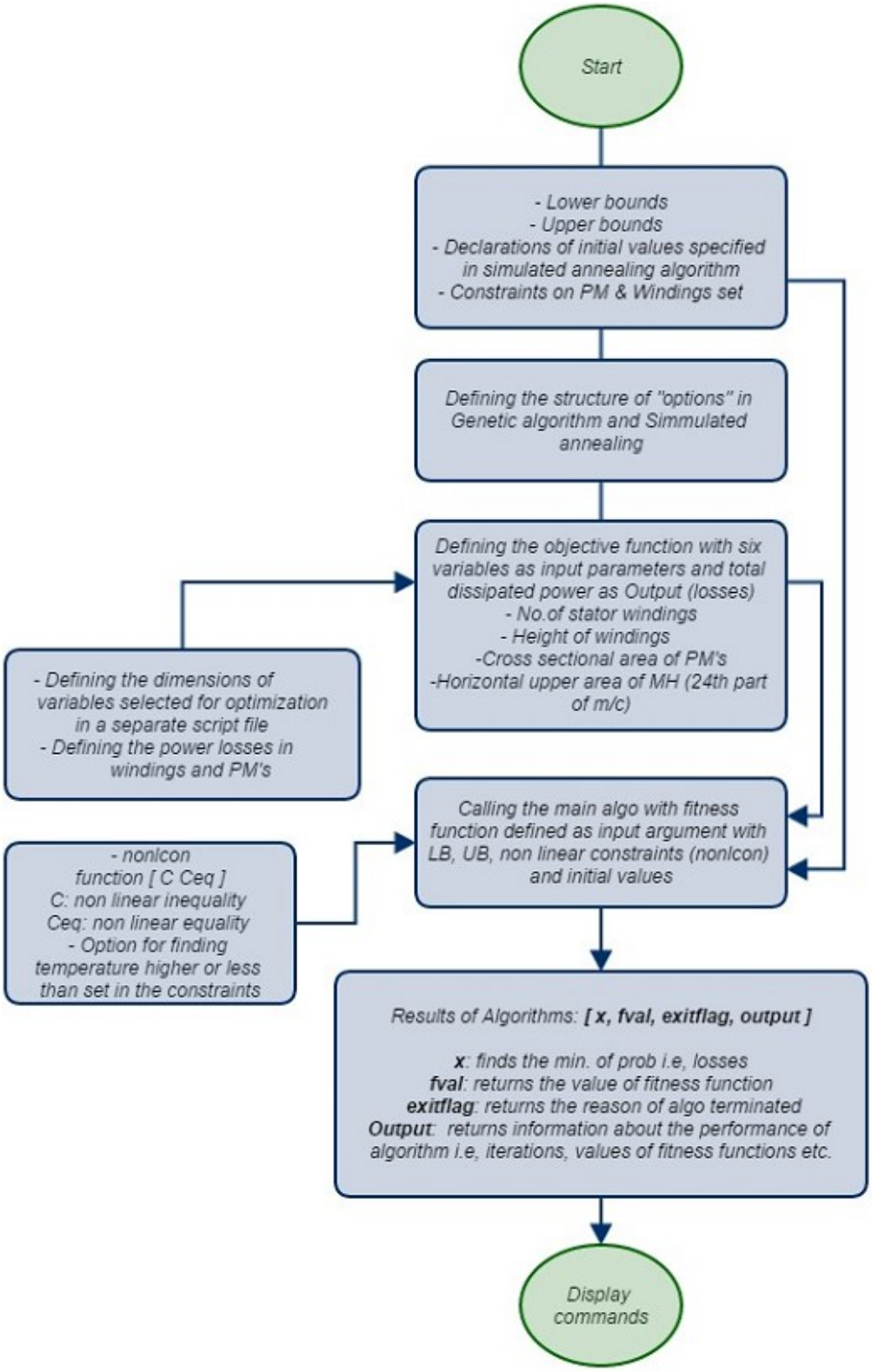

Figure 28: Flow chart of the code in Matlab ® for Structural Optimization of an electrical machine

5.3.1 Optimization Result of Unconstrained Genetic Algorithm

Optimization terminated: average change in the fitness value less than options.TolFun.

fval (Total dissipated power) = 57.4302 W, x =: [0.097367003 5.0000007 5.0000011 1.0160474e-005 1e-005 0.0077196038]

SOLUTION OF OPTIMIZATION (UNCONSTRAINED GENETIC ALGORITHM):

The number of generations was: 151

The number of function evaluations was: 228000

The best function value found was: 57.4302

Best L_W8: 0.097367

Best N2: 5

Best N3: 5

Best S_PM2: 1.01605e-005

Best S_PM3: 1e-005

Best S_MHu: 0.0077196

Temperature at W2i: 44.968 °C

Temperature at W3i: 45.7673 °C

Temperature at MH2: 44.3299 °C

Temperature at MH3: 44.9965 °C

Temperature at Rotor: 40.0836 °C

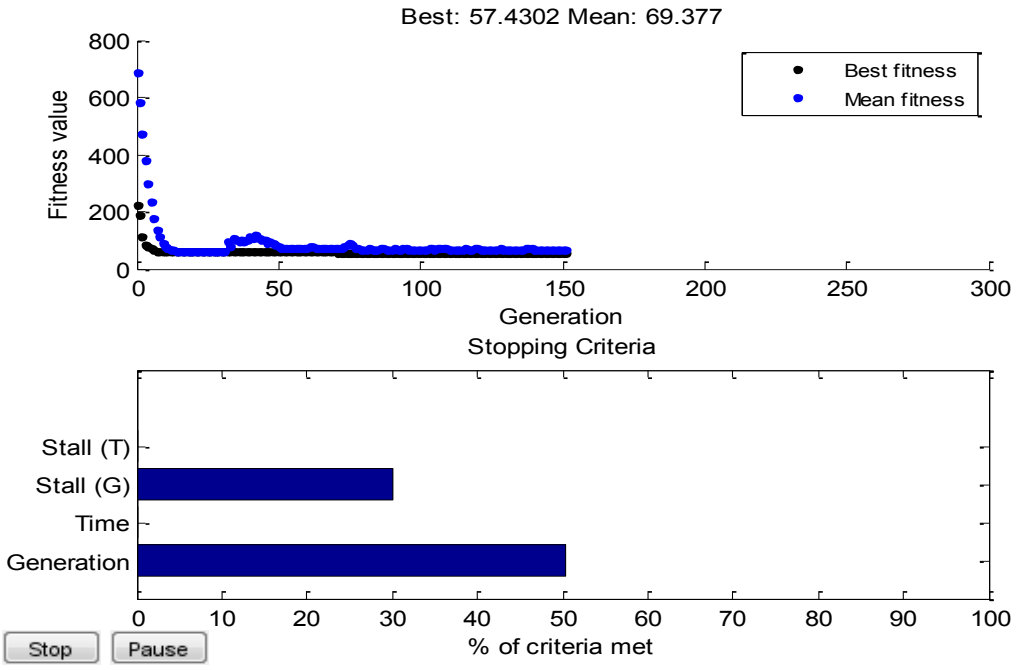

Figure 29: Figure representing the results from unconstrained genetic algorithm with the optimal value of the objective function found at 57.4302

5.3.2 Optimization Result of Constrained Genetic Algorithm

The optimization result for constrained genetic algorithm with constraints on temperature of permanent magnets and windings for finding the temperatures lower than the set ones ($T\_PMset = 80$ ℃ $and\ T\_Wset = 90$ ℃) is given below. It can clearly be seen from the results, that the maximum temperature on the permanent magnets and the windings are below the set ones and it describes the temperatures at specific regions with the corresponding values of the design variables.

Optimization terminated: average change in the fitness value less than options.TolFun and constraint violation is less than options.TolCon.

fval (Total dissipated power) = 57.2284 W, x =: [0.099999989 5 5 1.0006904e-005 1.0003382e-005 0.0099999925]

SOLUTION OF OPTIMIZATION (CONSTRAINED GENETIC ALGORITHM):

The number of generations was: 6

The number of function evaluations was: 343000

The best function value found was: 57.2284

Best L_W8: 0.09999

Best N2: 5

Best N3: 5

Best S_PM2: 1.00069e-005

Best S_PM3: 1.00034e-005

Best S_MHu: 0.00999999

Temperature at W2i: 44.3812 °C

Temperature at W3i: 45.327 °C

Temperature at MH2: 43.8244 °C

Temperature at MH3: 44.6182 °C

Temperature at Rotor: 40.0773 °C

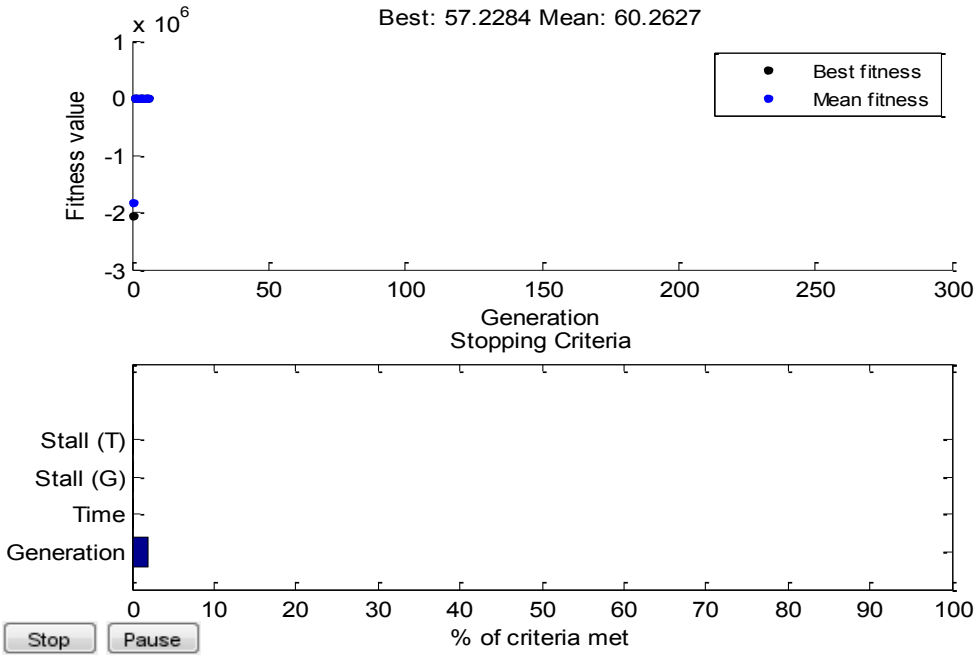

Figure 30: Figure representing the results from constrained genetic algorithm with the optimal value of the objective function found at 57.2284

5.3.3 Optimization Result of Simulated Annealing

Optimization terminated: change in best function value less than options.TolFun.

fval (Total dissipated power) = 57.2288 W, x =: [0.099613897 5.0436824 5.0007476 1e-005 1.0000004e-005 0.0075540996]

SOLUTION OF OPTIMIZATION (SIMULATED ANNEALING):

The number of iterations was: 4013

The number of function evaluations was: 4056

The best function value found was: 57.2288

Best L_W8: 0.0996139

Best N2: 5.04368

Best N3: 5.00075

Best S_PM2: 1e-005

Best S_PM3: 1e-005

Best S_MHu: 0.0075541

Temperature at W2i: 46.1378 °C

Temperature at W3i: 46.529 °C

Temperature at MH2: 45.3335 °C

Temperature at MH3: 45.6465 °C

Temperature at Rotor: 40.0947 °C

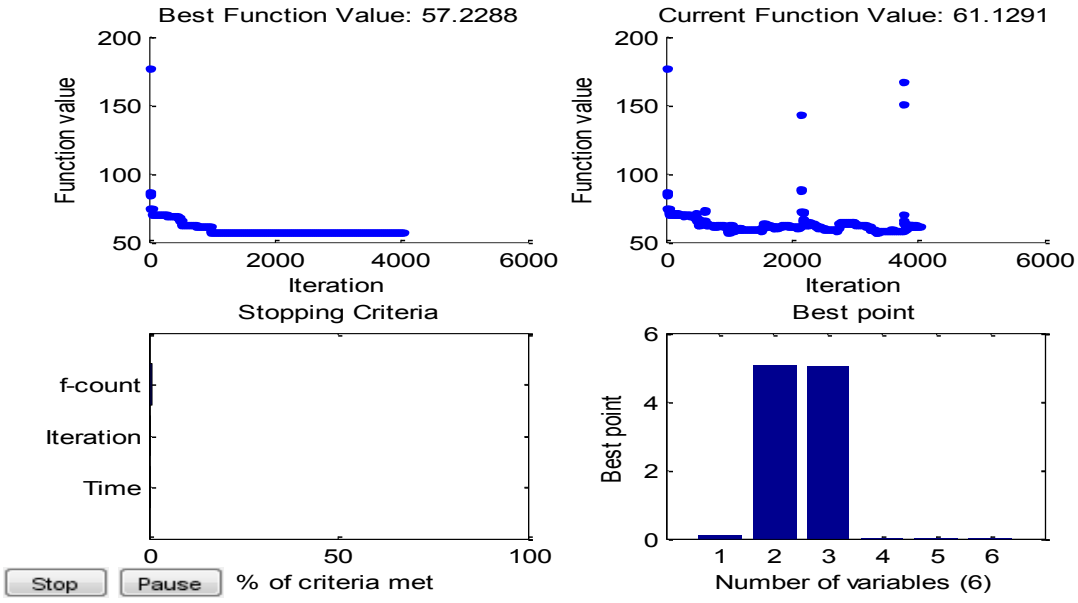

Figure 31 Figure representing the results from simulated annealing algorithm with the optimal value of the objective function found at 57.2288

It can be seen from the results of the optimization (Figure 29 – 31) that both the genetic algorithm and simulated annealing generates nearly the same results for the same parameters used in the objective function. The main task was to minimize the dissipated power i.e. the losses to maximize the efficiency and it can be seen that the best objective function value found in all the cases is roughly 57 W, when the input arguments to the objective function like the number of windings, height of the PM's etc. are at their optimal values. The slight differences in the values of some parameters are obvious from the fact that both the algorithms use random sampling methods to create random solutions.

By running the algorithm of constrained genetic optimization it can be seen that it is much slower in this case and gives nearly the same value of objective function as compared with the case of unconstrained optimization. An important point to mention here is that unconstrained optimization strives only to get low value of power dissipated as the objective function value, while constrained optimization also tries to limit the temperatures within bounds.

Also one more thing that is of importance in both the algorithms is that it is better to run these algorithms several times before arriving at a final conclusion. The reason is that since they are based on random generators in which we could get consistently different solutions using the same parameters.

We can replicate the results produced if we reset the states of arbitrary number generators by utilizing the data given by genetic algorithm or simulated annealing. Genetic algorithm gives the final condition of the random number generators. The data provided by the algorithms could then be utilized to bring the states back to original.

The OPTIMTOOL in Matlab ® gives the options to carry out experimentation and then comparing them by simulating with different solver techniques.

6 Conclusions

This report has explored the thermal behavior and structural optimization of FSPM machine. Other than getting genuine temperature forecast of the machine parts being referred to, it has been possible to address some vulnerability in the data information, essential observations while modeling thermal resistance network and most importantly what machine parameters ought to be taken into account while considering the optimal design.

Similar to other modeling techniques, thermal model is inherently questionable as even by spending a lot of time and resources in building a model and perform experiments, it might be hard to acquire faultless estimations for few parameters. In this report, all such estimations have been taken from similar comparable machines. But there are of course few drawbacks to these sorts of assumptions as almost every motor has different design concept and they also vary between individuals related to the same design group. Moreover, there are constraints which should be taken into account while considering the developed model, for example, the way how axial heat flows and the corresponding temperature, which have not been researched in great depth in the scope of this thesis.

Both analytical models as well as FEM simulations have this sort of uncertainty. However as the FEM simulations are considered more accurate because of the exact temperature prediction at the point of interest, they suffer from some serious drawbacks, including errors and limitations in input data and in the thermal model. The FEM-result can consequently not be considered as the reliable result in a manner that these simulations cannot compensate the actual measurements carried out during the experimentation phase. The definite number of the nodes introduced in the machine under investigation should not be viewed as the imperative section of the result rather what is important is perhaps pointing out the important machine parameters and the comprehensive explanation of thermal behavior of FSPM machine.

Windings are probably the most important part of the machine in the design of a motor as majority of losses in the form of heat starts to take place here which ultimately sets the upper limit constraints on the output power. The temperature in the windings is dependent on many factors which the designer has to consider as these parameters are difficult to estimate and accordingly constitutes an extensive instability in the model.

Air gap is considered one of the most important machine design part in terms of thermal accuracy and behavior of the FSPM machine. The most significant source of vulnerability, while considering the air gap is the turbulence of the air stream which requires simulations in computational fluid dynamics (CFD) medium and the effects of rotor expansion by thermal impact. As air has high thermal resistance, the air gap has a noticeable effect on the rotor temperature and makes it extremely delicate to increment in losses in the rotor.

Besides having detailed information about distinctive parts of the machine, some general techniques for thermal resistance network modeling have been inspected. Among these is the complete transient investigation by including thermal capacitances which provide an additional heat transfer path in dynamical states at different node points. It was found out that it requires nearly an hour for the temperatures to reach to their steady state values. For basic shapes with well characterized heat transfer paths, the analytical method of building a thermal model with resistances is found to be precise. But for more complicated shapes where the high temperature ways can differ more, the results have a tendency to be more estimated. One investigation where

the conclusion turned out to be the same as the proposed strategy was when examining the losses injected in the windings 2 with a distributed heat generation. Exact information of the losses is an essential for the accuracy of the model. The thesis work was not related to the calculation of the losses, so the model was limited to only the main measurements defined in the losses by the Joule's law and by the electromagnetic model.

The work of optimization presented in this thesis deals with an optimization based design of a FSPM machine. An optimization code for electrical machine has been proposed to maximize the efficiency and to minimize the losses. To achieve the design goals, an objective function has been created, the sensitivity of whose depends on the number of input arguments (variables). The genetic algorithm, based on the fitness function value, lower limits, upper limits and behavioral constraints, changes the genetics of the population to search for an optimal value from the search space. On the other hand, simulated annealing based on heating and cooling processes, accept new randomly created trial points by the process of Annealing and Reannealing.

As indicated by the examination and the displayed results, it might be presumed that the both the algorithms are exceptionally suitable for configuration and structural streamlining of FSPM machine and in general to all electrical machines. By utilizing Genetic calculation or Simulated Annealing the danger of trapping in a neighborhood maxima or minima is to a great degree diminished, which is exceptionally hard to eliminate with in deterministic systems.

6.1 Future Work

The thermal model described in the scope of this thesis covers most parts of the test machine, yet commonly there are things that need to be developed further. The most evident is the expansion of the nodes in the thermal resistance network to have deep insight knowledge of temperature distributions in different parts of the machine. This basically means including nodes for the end windings, the air and maybe for the motor case, bearings and so on. The heating of the cooling fluid and the effect of cooling method is something else that could be applicable to research. Furthermore, the effect of thermal temperatures on various parts can be investigated in more detail by including thermal capacitances nodes in the transient model to empower performing transient analysis in more detail.

At the time of writing of the thesis, the machine under investigation has become available for experimenting task and temperature measurements will be available soon. This will help to distinguish any frail spots in the network. Further tests on the machine will likewise enhance the input information of the machine utilized as a part of the software simulation. The most important thing that can be improved is the losses which we can have by mixing the strategies of the electromagnetic model and COMSOL Multiphysics ®. The suppositions and the use of symmetries made in the model can further be improved by contrasting it with experimental results. Finally at the end, the nature of the Genetic calculation or Simulated Annealing model can be improved by comparing it will FEM data analysis of the initial design of the motor and the optimized solution.

References

[1] G. Kylander. “Thermal Modeling of small cage induction motors". PhD Thesis, Chalmers University of Technology, 1995

[2] K&K Associates. Thermal Network Modeling Handbook version 97.003 Nation Aeronautics and Space Administration, 1976

[3] M. Kaufman. "Principles of Thermodynamics” CRC Press, 2002 ISBN: 978-0-203-90976-8

[4] Zhang. “*Radiative Transfer through Transparent Media”* July 2010.
URL: https://www.thermalfluidscentral.org / © 2010 – 2011, Global Digital Central

[5] J. Nerg, M. Rilla and J. Pyrhönen “Thermal Analysis of Radial-Flux Electrical Machines with High Power Density" In: Industrial Electronics, IEEE Transactions on 55.10 (2008), pp. 3543-3554. ISSN: 0278-0046. Doi: 10.1109/TIE.2008.927403

[6] R. L. Taylor, Zienkiewicz O. C. and J.Z. Zhu. The Finite Element Method: Its Basis and Fundamentals. Sixth Edition Butterworth-Heinemann, 2005

[7] Z. Kolondzovski, A. Belahcen, A. Arkkio, Multiphysics thermal design of a high-speed permanent-magnet machine, Applied Thermal Engineering (2009) , doi: 10.1016/j.applthermaleng.2009.01.001

[8] Comsol Multiphysics, Heat Transfer Module, User’s Guide, Version 3.3, 2006

[9] Eva Belicov´a and Val´eria Hrabovcov´a, Analysis of an axial flux permanent magnet machine (AFPM), based on coupling of two separated simulation models (electrical and thermal) Journal of ELECTRICAL ENGINEERING, VOL. 58, NO 1, 2007, 3–9

[10] Y.K. Chin, E. Nordlund, D.A. Staton, Thermal Analysis- Lumped-circuit model and Finite Element Analysis, Magna Physics Oxford Science Publications, 1994

[11] T.Jokinen, J.Saari, Modeling of the coolant flow with heat flow controlled temperature sources in thermal networks, IEE Proc.-Electr. Power Appl., Vol. 144, No 5, September 1997, IEE Proceedings online no. 19971384

[12] Naghi Rostami, Mohammad Reza Feyzi, Juha Pyrhönen, Asko Parviainen, Markku Niemelä, Lumped-Parameter Thermal Model for Axial Flux Permanent Magnet Machines, IEEE TRANSACTIONS ON MAGNETICS, VOL. 49, NO. 3, MARCH 2013

[13] J. F. Gieras, R. J. Wing and M. J. Kamper*, Axial-Flux Permanent Magnet Machines,* Dordrecht, The Netherlands: Kluwer, 2004, p.340

[14] A. Bousbaine, M. McCorrnick, W.F. Low, IN-SITU DETERMINATION OF THERMAL COEFFICIENTS FOR ELECTRICAL MACHINES, EEE Transactions on Energy Conversion, Vol. 10, No. 3, September 1995

[15] E. Ilhan, M. F. J. Kremers, T. E. Motoasca, J. J. H. Paulides and E. Lomonova, Transient Thermal Analysis of Flux Switching PM machines, 2013 Eighth International Conference and Exhibition on Ecological Vehic1es and Renewable Energies (EVER)

[16] Gazley, C. 'Heat Transfer Characteristics of rotating and axial flow between concentric cylinders', Trans ASME, pp.79-89. Jan 1958

[17] P.H. Mellor, D. Roberts, D.R. Turner, Lumped parameter thermal model for electrical machines of TEFC design, IEE PROCEEDINGS-B, Vol. 138, No. 5, SEPTEMBER 1991

[18] Janne Nerg, Marko Rilla, Juha Pyrhönen, Thermal Analysis of Radial-Flux Electrical Machines With a High Power Density, IEEE TRANSACTIONS ON INDUSTRIAL ELECTRONICS, VOL. 55, NO. 10, OCTOBER 2008

[19] Kaltenbacher, M., Saari, J. 1992. An asymmetric thermal model of totally enclosed fan-cooled induction motors, Report 38, Helsinki university of Technology, Laboratory of Electro mechanics, Espoo, Finland, 62p

[20] Ari Haavisto, Thermal model of axial flux permanent magnet machine, Master of Science thesis, Helsinki university of Technology, Laboratory of Electro mechanics, Espoo, Finland, 2006

[21] BJORN ANDERSSON, Lumped Parameter Thermal Modeling of Electric Machines, Analysis of an Interior Permanent Magnet Synchronous, Machine for Vehicle Applications, Master of Science thesis, Chalmers university of technology, Goteborg, Sweden, 2013

[22] Lyudmila Popova, COMBINED ELECTROMAGNETIC AND THERMAL DESIGN PLATFORM FOR TOTALLY ENCLOSED INDUCTION MACHINES, Master of Science thesis, LAPPEENRANTA UNIVERSITY OF TECHNOLOGY, Lappeenranta, May 20, 2010

[23] Joachim Lindstrom, Thermal Model of permanent-Magnet Motor for hybrid electric Vehicle, Master of Science thesis, Chalmers university of technology, Goteborg, Sweden, 1999

[24] Aldo Boglietti, Andrea Cavagnino, David Staton, Martin Shanel, Markus Mueller, and Carlos Mejuto, Evolution and Modern Approaches for Thermal Analysis of Electrical Machines, IEEE TRANSACTIONS ON INDUSTRIAL ELECTRONICS, VOL. 56, NO. 3, MARCH 2009

[25] http://www.thermopedia.com/content/874/ Date of reference 02.02.2011

[26] Luke, G.F. The cooling of electric machines', *Trans. AIEE,* 45, pp. 1278-1288, 1923

[27] Dmitry Svechkarenko, Thermal Modeling and Measurements of Permanent Magnet Machines, Master Thesis, Royal Institute of Technology, Department of Electrical Engineering, Electrical Machines and Power Electronics, Stockholm 2004

[28] F. Kreith, M.B. Bohn, Principles of Heat Transfer, 5th ed., ISBN 0-534-95420- 0, PWS Publishing Company, Boston, 1997

[29] B.Sareni, L.Krahenbuhl and A.Nicolas, "Niching Genetic Algorithms for Optimization in Electro-magnetics". The 11th COMPUMAG'97, pp.563-564, Rio de Janeiro, 1997

[30] http://www.mathworks.se/help/gads/what-is-the-genetic-algorithm.html/ © 1994 - 2014, The MathWorks, Inc

[31] http://www.mathworks.se/help/gads/what-is-simulated-annealing.html / © 1994 - 2014, The MathWorks, Inc

[32] "Dimensionless quantity" *Wikipedia: the Free Encyclopedia*. Wikimedia Foundation, Inc. June 2013. Web. 10 Aug. 2014. <http://en.wikipedia.org/wiki/Dimensionless_quantity>

[33] Guangjin Li, *Student Member, IEEE*, Javier Ojeda, *Member, IEEE*, Emmanuel Hoang, Mohamed Gabsi, *Member, IEEE*, and Michel Lécrivain, Thermal–Electromagnetic Analysis for Driving Cycles of Embedded Flux-Switching Permanent-Magnet Motors, IEEE TRANSACTIONS ON VEHICULAR TECHNOLOGY, VOL. 61, NO. 1, JANUARY 2012

[34] Li Hao, Mingyao Lin, Wan Li, Hao Luo, Xinghe Fu and Ping Jin, Novel Dual-Rotor Axial Field Flux-Switching Permanent Magnet Machine, IEEE TRANSACTIONS ON MAGNETICS, VOL. 48, NO. 11, NOVEMBER 2012